

# Quarterly Technical Report

## Selected Energy Epitaxial Deposition and Low Energy Electron Microscopy of AlN, GaN and SiC Thin Films

Supported under Grant #N00014-95-1-0122  
Office of the Chief of Naval Research  
Report for the period 7/1/97-9/30/97

**DISTRIBUTION STATEMENT B**

Approved for public release  
Distribution Unlimited

**DTIC QUALITY INSPECTED 2**

R. F. Davis, H. H. Lamb<sup>†</sup> and I. S. T. Tsong\*,  
E. Bauer\*, E. Chen<sup>†</sup>, R. B. Doak\*, J. L. Edwards\*,  
N. Freed\*, J. Fritsch\*, D. C. Jordan\*, A. Michel<sup>†</sup>,  
A. Pavlovska\*, K. E. Schmidt\*, and V. Torres\*  
Materials Science and Engineering Department

<sup>†</sup>Chemical Engineering  
North Carolina State University  
Campus Box 7907  
Raleigh, NC 27695-7907

and  
\*Department of Physics and Astronomy  
Arizona State University  
Tempe, AZ 85287-1504

19971203 146

September, 1997

REPORT DOCUMENTATION PAGE			Form Approved OMB No. 0704-0188	
Public reporting burden for this collection of information is estimated to average 1 hour per response, including the time for reviewing instructions, searching existing data sources, gathering and maintaining the data needed, and completing and reviewing the collection of information. Send comments regarding this burden estimate or any other aspect of this collection of information, including suggestions for reducing this burden to Washington Headquarters Services, Directorate for Information Operations and Reports, 1215 Jefferson Davis Highway, Suite 1204, Arlington, VA 22202-4302, and to the Office of Management and Budget Paperwork Reduction Project (0704-0188), Washington, DC 20503.				
1. AGENCY USE ONLY (Leave blank)		2. REPORT DATE September, 1997		3. REPORT TYPE AND DATES COVERED Quarterly Technical 7/1/97-9/30/97
4. TITLE AND SUBTITLE Selected Energy Epitaxial Deposition and Low Energy Electron Microscopy of AlN, GaN, and SiC Thin Films			5. FUNDING NUMBERS 1213801---01 312 N00179 N66020 4B855	
6. AUTHOR(S) R. F. Davis, H. H. Lamb and I. S. T. Tsong				
7. PERFORMING ORGANIZATION NAME(S) AND ADDRESS(ES) North Carolina State University Hillsborough Street Raleigh, NC 27695			8. PERFORMING ORGANIZATION REPORT NUMBER N00014-95-1-0122	
9. SPONSORING/MONITORING AGENCY NAMES(S) AND ADDRESS(ES) Sponsoring: ONR, Code 312, 800 N. Quincy, Arlington, VA 22217-5660 Monitoring: Administrative Contracting Officer, Regional Office Atlanta Atlanta Regional Office 100 Alabama Street, Suite 4R15 Atlanta, GA 30303			10. SPONSORING/MONITORING AGENCY REPORT NUMBER	
11. SUPPLEMENTARY NOTES				
12a. DISTRIBUTION/AVAILABILITY STATEMENT Approved for Public Release; Distribution Unlimited			12b. DISTRIBUTION CODE	
13. ABSTRACT (Maximum 200 words) The kinematic conditions under which III-Nitrides films can be grown were determined using efficient local-orbital molecular-dynamics simulations. Reaction paths for the impact of ammonia molecules on the cation- and anion-terminated surfaces of GaN and AlN were also determined. <i>In situ</i> growth experiments of GaN on 6H-SiC(0001) substrates were conducted in the low-energy electron microscope (LEEM). Initial nucleation at the steps and subsequent growth across the terraces were observed. The LEED patterns indicated three-dimensional crystal growth with pronounced formation of facets. Such growth behavior occurred irrespective of the method of deposition. A seeded beam source chamber has been interfaced with a UHV deposition chamber. Films of AlN have been grown with this system. Smooth, homoepitaxial GaN films were grown using an effusive Ga source and an NH <sub>3</sub> -seeded supersonic molecular beam. A small Ga flux-substrate temperature window was found that allows for two-dimensional homoepitaxial growth under MBE-like conditions ( $T_s=730^\circ\text{C}$ , $P_b=2\times 10^{-6}$ Torr). Mass-analyzed Ga <sup>+</sup> , N <sub>2</sub> <sup>+</sup> and N <sup>+</sup> ions at ~20 eV with a small energy spread of ~1 eV at FWHM were produced via two Colutron units with deceleration lenses. Ion beams of N <sub>2</sub> <sup>+</sup> and N <sup>+</sup> were used to perform nitridation of Si(100) surfaces. Subsequent SIMS depth profiles indicated the presence of nitride layers on the Si(100) substrates. Codeposition of Ga and N on Si(111) and Si(100) substrates was conducted with the Ga <sup>+</sup> and N <sub>2</sub> <sup>+</sup> ion beams. SIMS depth profiles showed the presence of both Ga and N on the Si substrate surfaces suggesting the formation of a GaN layer. A second generation arc-heated jet source and an inexpensive corona discharge source were designed, fabricated and characterized. Preliminary optical spectra of these sources were obtained and evaluated. An improved optical and electronic system has been designed and is being assembled. It will allow spatially resolved spectroscopy of the plasma expansion to be made at various points downstream of the nozzle, thereby monitoring changes in excited state population in the free-jet expansion.				
14. SUBJECT TERMS GaN, AlN, SiC, kinematic conditions, reaction paths, low energy electron microscope, low energy electron diffraction, LEEM, LEED, seeded beam, homoepitaxial growth, SIMS, Colutron, arc-heated jet, corona discharge, optical spectra, free-jet expansion			15. NUMBER OF PAGES 37	
			16. PRICE CODE	
17. SECURITY CLASSIFICATION OF REPORT UNCLAS	18. SECURITY CLASSIFICATION OF THIS PAGE UNCLAS	19. SECURITY CLASSIFICATION OF ABSTRACT UNCLAS	20. LIMITATION OF ABSTRACT SAR	

## Table of Contents

I.	Introduction	1
II.	<i>Ab initio</i> Calculation of the Structure and Growth Properties of the III-V Nitrides	4
III.	<i>In Situ</i> Real-Time Studies of GaN Growth on 6H-SiC(0001) by Low-Energy Electron Microscopy (LEEM)	6
IV.	Effects of Energy and Angle of Incidence on AlN and GaN Epitaxial Growth using Helium Supersonic Beams Seeded with NH <sub>3</sub>	15
V.	Homoepitaxial Growth of Stoichiometric GaN Films using an Ammonia-seeded Supersonic Beam	18
VI.	Deposition of GaN Thin Films by Dual Low-energy Ion Beams	26
VII.	Arc-Heated Supersonic Free-Jet of Nitrogen Atoms for the Growth of GaN, AlN and InN Thin Films	34
VIII.	Distribution List	37

## I. Introduction

The realized and potential electronic applications of AlN, GaN and SiC are well known. Moreover, a continuous range of solid solutions and pseudomorphic heterostructures of controlled periodicities and tunable bandgaps from 2.3 eV (3C-SiC) to 6.3 eV (AlN) have been produced at North Carolina State University (NCSU) and elsewhere in the GaN-AlN and AlN-SiC systems. The wide bandgaps of these materials and their strong atomic bonding have allowed the fabrication of high-power, high-frequency and high-temperature devices. However, the high vapor pressures of N and Si in the nitrides and SiC, respectively, force the use of low deposition temperatures with resultant inefficient chemisorption and reduced surface diffusion rates. The use of these low temperatures also increases the probability of the uncontrolled introduction of impurities as well as point, line and planar defects which are likely to be electrically active. An effective method must be found to routinely produce intrinsic epitaxial films of AlN, GaN and SiC having low defect densities.

Recently, Ceyer [1, 2] has demonstrated that the barrier to dissociative chemisorption of a reactant upon collision with a surface can be overcome by the translational energy of the incident molecule. Ceyer's explanation for this process is based upon a potential energy diagram (Fig. 1) similar to that given by classical transition-state theory (or activated-complex theory) in chemical kinetics. The dotted and dashed lines in Fig. 1 show, respectively, the potential wells for molecular physisorption and dissociative chemisorption onto the surface. In general, there will be an energy barrier to overcome for the atoms of the physisorbed molecule to dissociate and chemically bond to the surface. Depending upon the equilibrium positions and well depths of the physisorbed and chemisorbed states, the energy of the transition state  $E^*$  can be less than zero or greater than zero. In the former case, the reaction proceeds spontaneously. In the latter case, the molecule will never proceed from the physisorbed state (the precursor state) to the chemisorbed state unless an additional source of energy can be drawn upon to surmount the barrier. This energy can only come from either (1) the thermal energy of the surface, (2) stored internal energy (rotational and vibrational) of the molecule, or (3) the incident translational kinetic energy of the molecule. Conversion of translational kinetic energy into the required potential energy is the most efficient of these processes. Moreover, by adjusting the kinetic energy,  $E_i$ , of the incoming molecule, it is possible to turn off the reaction ( $E_i < E^*$ ), to tailor the reaction to just proceed ( $E_i = E^*$ ), or to set the amount of excess energy to be released ( $E_i > E^*$ ). The thrust of the present research is to employ these attributes of the beam translational energy to tune the reaction chemistry for wide bandgap semiconductor epitaxial growth.

The transition state,  $E^*$ , is essentially the activation energy for dissociation and chemisorption of the incident molecules. Its exact magnitude is unknown, but is most certainly

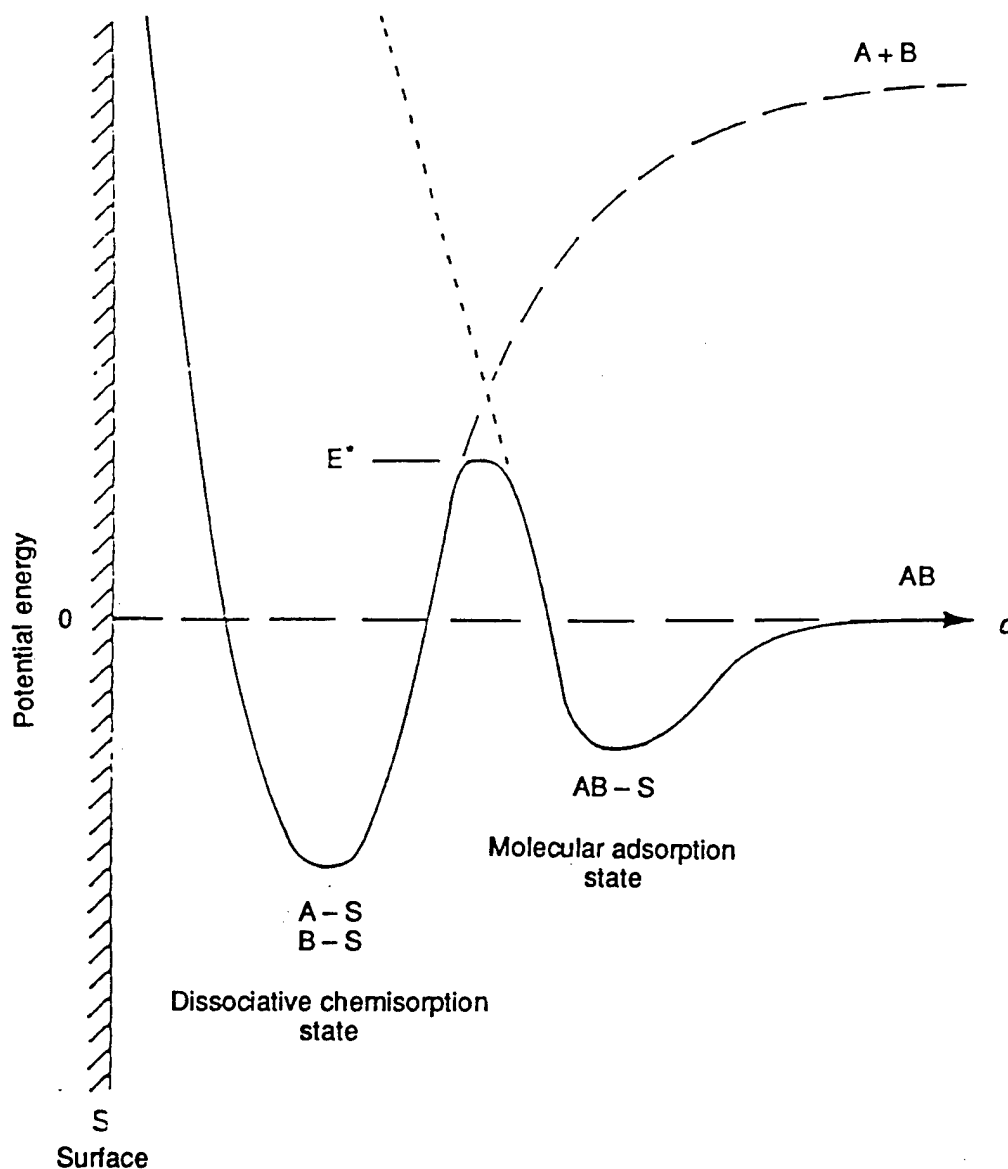


Figure 1. Schematic potential energy diagram of an activated surface reaction involving a molecularly physisorbed precursor state [from Ref. 1].

lower than the dissociation energy of the free molecule. It does not necessarily follow, however, that any kinetic energy above  $E^*$  will promote high-quality epitaxial growth of GaN. One must take into consideration another energy threshold,  $E_d$ , beyond which the kinetic energy of the incident flux will cause damage to the epitaxial film being synthesized. A typical  $E_d$  threshold value is approximately five times the bandgap of the crystal and in the case of GaN,  $E_d \approx 18$  eV.

From the above consideration, it is clear that the key to high quality epitaxial growth is to be able to tune the energy of the incoming flux species over a range of energies defined by the window between  $E^*$  and  $E_d$ . Since the window is quite restrictive, i.e. 1-20 eV, it is essential that the energy spread of the flux species must be small, i.e. the flux species should ideally be

monoenergetic. To this end, we employ Selected Energy Epitaxial Deposition (SEED) systems for the growth of AlN, GaN and SiC wide bandgap semiconductors. The SEED systems are of two types: (1) a seeded-beam supersonic free-jet (SSJ) and (2) a dual ion-beam Colutron. Both these SEED systems have the desirable property of a narrow energy spread of  $\leq 1$  eV.

Epitaxial growth using the seeded-beam SSJ involves a close collaboration between investigators at NCSU and Arizona State University (ASU). At ASU, the SSJ is interfaced directly into a low-energy electron microscope (LEEM) for the conduct of *in situ* studies of the nucleation and growth of epitaxial layers; while at NCSU, the SSJ systems are used to grow device-quality AlN, GaN and SiC for real applications. Exchanges in personnel (students) and information between the two groups ensures the achievement of desired results. The additional thin film growth experiments using dual-beam Colutrons and the theoretical studies referred to in this report are primarily conducted at ASU.

The research conducted in this reporting period and described in the following sections has been concerned with (1) kinematic conditions under which III-nitrides films can be grown, (2) reaction paths for the impact of ammonia molecules on the cation- and anion-terminated surfaces of GaN and AlN, (3) *in situ* growth experiments of GaN on 6H-SiC(0001) substrates in the low-energy electron microscope (LEEM), (4) growth of homoepitaxial GaN films using an effusive Ga source and an NH<sub>3</sub>-seeded supersonic molecular beam, (5) production of mass-analyzed Ga<sup>+</sup>, N<sub>2</sub><sup>+</sup> and N<sup>+</sup> ions at ~20 eV with a small energy spread of ~1 eV at FWHM via two Colutron units and (6) design, fabrication and characterization of a second generation arc-heated jet source and an inexpensive corona discharge source. The following individual sections detail the procedures, results, discussions of these results, conclusions and plans for future research. Each subsection is self-contained with its own figures, tables and references.

1. S. T. Ceyer, Langmuir 6, 82 (1990).
2. S. T. Ceyer, Science 249, 133 (1990).

## II. *Ab initio* Calculation of the Structure and the Growth Properties of the Group-III Nitrides

In the first phase of our work, the bulk and surface properties of GaN and AlN was characterized to carefully evaluate the accuracy of the local-orbital *ab initio* formalism [1, 2] used in our calculations. The computed bulk lattice constants, bulk phonon frequencies, surface relaxations and total energies of the polar and non-polar surfaces of GaN and AlN [3] were in excellent agreement with the results from highly converged plane-wave pseudopotential calculations [4, 5, 6, 7, 8]. By means of an efficient *ab initio* scheme, kinematic conditions were investigated which were suitable for effectively growing thin Group-III nitride films. In order to study the initial stages of the epitaxial deposition, reaction paths we determined for the impact of ammonia molecules on the cation- and anion-terminated surfaces of GaN and AlN. Initial results indicated that the dissociation of  $\text{NH}_3$  followed by the adsorption of nitrogen and hydrogen on the surface was exothermic. To understand in more detail the energetics of such surface chemical reactions and to identify possible reaction products, an ammonia molecule approaching the anion-terminated (0001) surface of wurtzite-phase GaN was first considered. The total energy was computed as a function of the molecule's distance from the surface, for which the stable nitrogen-vacancy configuration was assumed. All atoms in the system were allowed to relax. The interaction of  $\text{NH}_3$  with GaN was analyzed by monitoring the total energy for all configurations, the surface induced reorientation and deformation of the molecule, as well as atomic relaxations in the growing film.

In this way, information was obtained about active adsorption sites, the reaction path, and the energy barriers for the incorporation of nitrogen into the growing film. An important question was focused on the role of hydrogen during the growth. Is hydrogen incorporated into the surface and how large is the probability for the dissociation of  $\text{NH}_3$  close to the surface? By probing the potential energy surface on the basis of total energy calculations for static configurations, an estimate was achieved for the energy which was necessary to desorb hydrogen and the energy gain from the incorporation of nitrogen into the surface. Moreover, the dynamical processes associated with the impact of ammonia was monitored by performing molecular dynamics simulations for various collision energies and incident angles of  $\text{NH}_3$ .

In order to investigate the initial growth induced by the deposition of ammonia to the full extent, various scenarios and configurations were considered. Differences in the surface structure and stoichiometry led to modifications in the adsorption process. Detailed analysis of total energies and the height of dissociation barriers, preferential adsorption configurations and/or surface areas were identified, including an estimate for sticking coefficients and growth rates. The deposition of nitrogen on the anion-terminated surface differed significantly from

that on the cation-terminated surface. Therefore, growth rates and epitaxial quality were expected to vary with the growth front.

Beside the dissociation of ammonia, which results from the molecule's impact on the surface, diffusion and mobility of atoms and molecules in the deposited layers were important processes that influenced the quality of the deposited films. To simulate the gross aspects of surface growth, including island formation, faceting, and the appearance of stacking faults, Monte Carlo simulations were used. Such calculations typically were based on rate constants which have been known for the arrival, sticking, and diffusion of the deposited particles. While simulations for many time steps and thousands of atoms were not feasible within *ab initio* calculations, short period molecular dynamics simulations based on the local orbital formalism were well suited to extract all of the important parameters like the mobility of adatoms and vacancies on the surface and their average diffusion length as a function of the temperature.

#### References

1. O. F. Sankey and D. J. Niklewski, Phys. Rev. B **40**, 3979 (1989).
2. A. A. Demkov, J. Ortega, O. F. Sankey, and M. Grumbach, Phys. Rev. B **52**, 1618 (1995).
3. J. Fritsch, O. F. Sankey, K. E. Schmidt, and J. B. Page, submitted to Phys. Rev. B.
4. A. F. Wright and J. S. Nelson, Phys. Rev. B **50**, 2159 (1994).
5. I. Gorczyka, N. E. Christensen, E. L. Peltzer y Blancá, and C. O. Rodriguez, Phys. Rev. B **51**, 11936 (1995).
6. K. Miwa and A. Fukumoto, Phys. Rev. B **48**, 7897 (1993).
7. J. E. Northrup and J. Neugebauer, Phys. Rev. B **53**, R10477 (1996); J. E. Northrup, R. di Felice, and J. Neugebauer, Phys. Rev. B **55**, 13878 (1997).
8. K. Kádas, S. Alvarez, E. Ruiz, and P. Alemany, Phys. Rev. B **53**, 4933 (1996).



### III. *In Situ* Real-Time Studies of GaN Growth on 6H-SiC(0001) by Low-Energy Electron Microscopy (LEEM)

A. Pavlovskaya, E. Bauer, V.M. Torres, J.L. Edwards, R.B. Doak and I.S.T. Tsong\*  
Department of Physics and Astronomy, Arizona State University, Tempe, AZ 85287-1504, USA

\*Tel: (602) 965-3563; Fax: (602) 965-7954; E-mail: ig.tsong@asu.edu

V. Ramachandran and R.M. Feenstra  
Department of Physics, Carnegie Mellon University, Pittsburgh, PA 15213, USA

#### Abstract

We report *in situ* growth experiments of GaN on 6H-SiC(0001) substrates conducted in the low-energy electron microscope (LEEM). The Ga flux species were supplied by an evaporative source while the nitrogen was supplied by either a N-atom RF plasma source or a supersonic seeded-beam jet (SSJ) source. The surfaces of the 6H-SiC(0001) substrates were prepared by high-temperature hydrogen etching prior to installation in the LEEM for deposition. On regions of the substrate surface where well-defined steps and terraces were observed, the LEEM video images showed initial nucleation at the steps and subsequent growth across the terraces. The LEED patterns indicated three-dimensional crystal growth with pronounced formation of facets. Such growth behavior occurred irrespective of the method of deposition.

## A. Introduction

Over the past decade or so, intense research efforts have been directed to the studies of Group III nitrides GaN, AlN, InN and their alloys in the form of epitaxial films because they can be used to fabricate short-wavelength light emitting diodes and laser diodes as well as high-power, high-frequency and high-temperature electronic devices [1-4]. In spite of these successful applications, optimization of the epitaxial growth process of the nitride films is still in progress in terms of reduction of defect densities and impurities, and lowering of substrate temperatures during deposition. In this report, we describe *in situ* real-time observations of GaN film growth which took place in a low-energy electron microscope (LEEM). We employed two methods of deposition: (a) the conventional MBE method where the Ga flux was supplied by an evaporative source and the N flux from a N-atom RF plasma source; and (b) the selected energy epitaxy (SEE) method where the Ga flux came from an evaporative source and the N source originated from a He supersonic beam seeded with NH<sub>3</sub>.

The SEE approach has the advantage of fine-tuning an energy window in which dissociation and reaction are promoted, surface diffusion is enhanced, while defect creation is minimized. All of these processes can, in principle, occur at a lower growth temperature since part of the translational energy of the flux species is converted into potential energy to overcome the activation barrier while the other part is manifested in the increase of surface mobility for the flux species to migrate to preferred sites such as step edges. It is essential that the energy spread of the flux species is small, i.e. a restrictive energy window to eliminate the high-energy tail, so that no damage will occur. The concept of a reactant overcoming the barrier to dissociative chemisorption by its translational energy upon collision with a surface has been demonstrated by Ceyer [5,6]. We have recently shown that monoenergetic beams in the energy range 0.20 to 0.65 eV produced by seeding a supersonic He beam with NH<sub>3</sub> can adequately serve this purpose [7,8].

## B. Experimental Procedure

The details of configuration and operation of our LEEM have been given previously by Bauer [9]. The Ga evaporative source and the Oxford Applied Research N-atom RF plasma source were mounted directly on the LEEM sample chamber at 16° incident angle to the substrate surface. A schematic diagram of the supersonic seeded-beam jet (SSJ) source is shown in Fig. 1, and this was attached to the LEEM sample chamber via a gate valve, also at an incident angle of 16°. Considerable efforts were devoted to minimizing the vibrations caused by the large mechanical pumps in the SSJ. The base pressure in the LEEM was below  $1 \times 10^{-10}$  Torr. The pressure rose to  $\sim 1 \times 10^{-5}$  Torr when the RF plasma source was in operation and to  $3 \times 10^{-8}$  Torr when the SSJ was used.

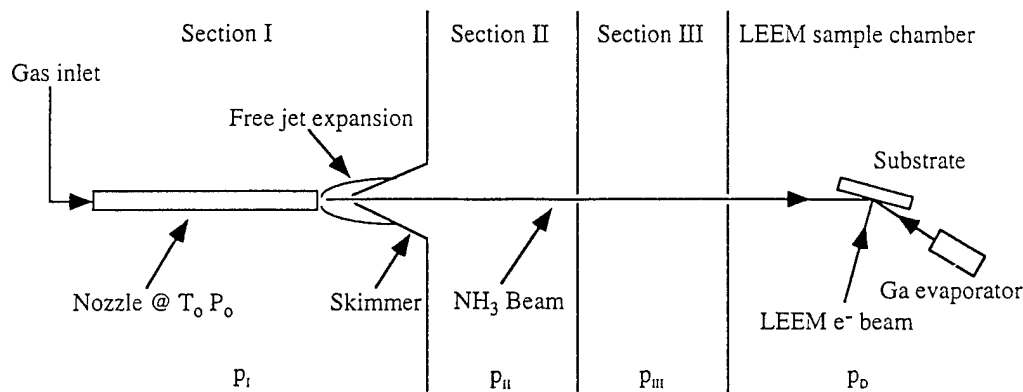


Figure 1. Schematic diagram of the SSJ source connected to the LEEM sample chamber for GaN growth. Pressures during deposition:  $P_0 = 1000$  Torr;  $p_I = 5 \times 10^{-4}$  Torr;  $p_{II} = 1 \times 10^{-6}$  Torr;  $p_{III} = 1 \times 10^{-7}$  Torr; and  $p_D = 3 \times 10^{-8}$  Torr.

The Ga evaporation rate was calibrated by observing in the LEEM the time taken for the conversion of Si(111)-(7 $\times$ 7) to Si(111)-( $\sqrt{3} \times \sqrt{3}$ )Ga which requires 1/3 ML Ga coverage [10]. The N flux from the N-atom RF plasma source was calibrated by LEEM observation of complete conversion of Si(111)-(7 $\times$ 7) to Si(111)-(8 $\times$ 8)N which requires 0.84 ML coverage of nitrogen [11]. The same procedure was repeated for the He supersonic beam seeded with 10% NH<sub>3</sub> to calibrate the NH<sub>3</sub> flux. Note that this flux actually reflects the number of N atoms reacting with the Si(111) surface after the dissociation of NH<sub>3</sub>. However, the dissociation rate may be different between the Si(111)-(7 $\times$ 7) surface used for calibration and the 6H-SiC(0001) surface used as a substrate.

From the deposition experiments with the RF plasma source, the substrate was held at 650°C, and the flux rates were ~3 ML/min for Ga and 0.5 ML/min for N with RF power at 200 W. The flux rates were essentially the same for deposition with the SSJ, although pitot measurements of the NH<sub>3</sub> flux [12] yielded ~5 ML/min, suggesting that only 1 out of 10 NH<sub>3</sub> molecules dissociate upon striking the surface. The substrate temperature for the SSJ deposition was 690°C.

### C. Results and Discussion

The 6H-SiC(0001) substrates were etched in a hydrogen atmosphere at 1600°C to remove polishing scratches. The LEEM image of such an etched surface is shown in Fig. 2, showing a regular array of steps and terraces. The step height is 15 Å as measured by atomic force microscopy (AFM), which is one unit cell for the 6H-SiC material. The LEED pattern of the etched surface in Fig. 2 shows clear (1 $\times$ 1) and ( $\sqrt{3} \times \sqrt{3}$ ) R30° structures. Unfortunately, not all 6H-SiC(0001) surfaces exhibit the same surface morphology after etching. Most show some small ordered regions with step structures and large disordered regions without any recognizable crystal structures. The lack of homogeneity of the SiC substrates obviously influences the growth modes and the film structure.

The growth of GaN on the substrate shown in Fig. 2 by the RF plasma source is shown by the frame-captured LEEM video images in Fig. 3. As soon as the substrate surface was exposed to the Ga and N fluxes, nucleation began at the step edges. Growth of the GaN crystal spread across the terraces slowly. Even after 2 hours, the film surface did not appear continuous, showing gaps on the surface.

The growth of GaN using the  $\text{NH}_3$  seeded beam from the SSJ source is shown in the LEEM images in Fig. 4. The initial 6H-SiC(0001) substrate shows a small ordered region with

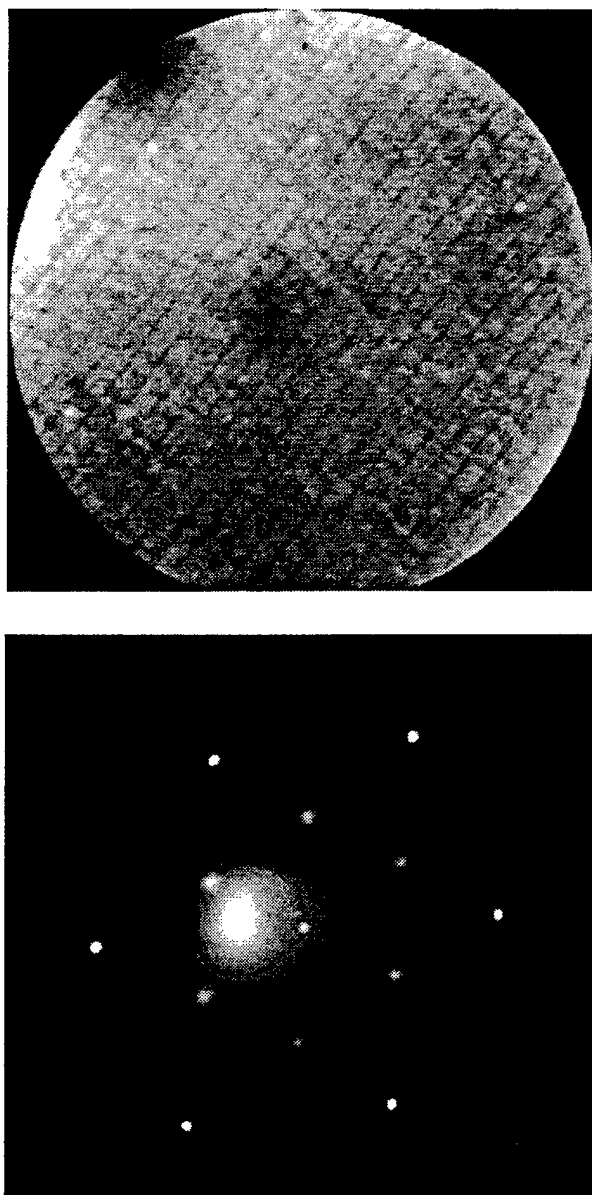


Figure 2. (Top) LEEM image of a hydrogen-etched 6H-SiC(0001) surface. Field of view  $4.8\ \mu\text{m}$ , electron energy 5.9 eV. (Bottom) LEED pattern of the surface above. Electron energy 22.8 eV.

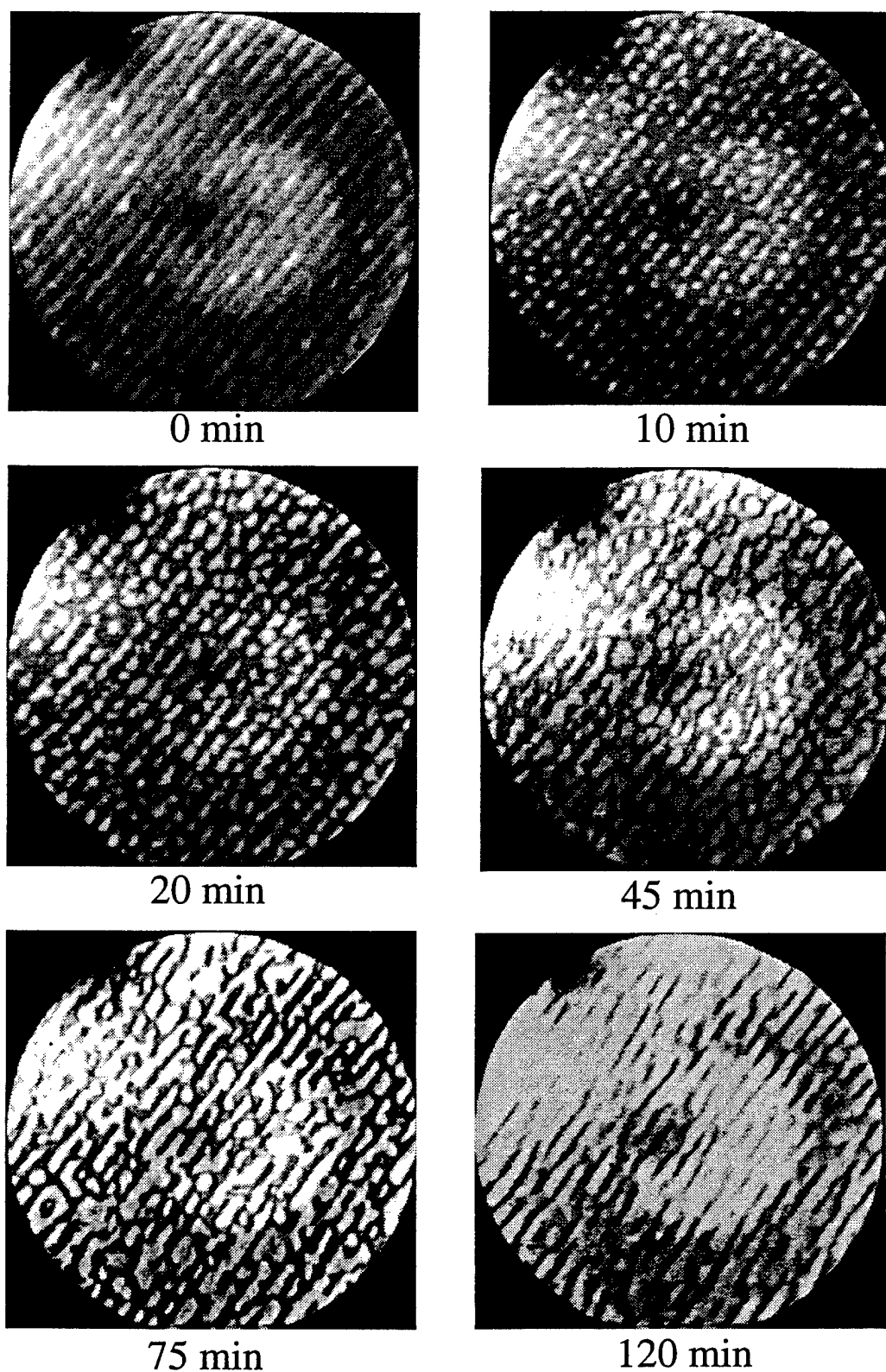


Figure 3. LEEM video images showing the growth of GaN by Ga evaporative source and N-atom RF plasma source on the 6H-SiC(0001) substrate shown in Fig. 2. Substrate temperature was 650°C. Time elapsed during deposition is indicated under each frame. Field of view 4.8  $\mu\text{m}$ , electron energy 6.6 eV.

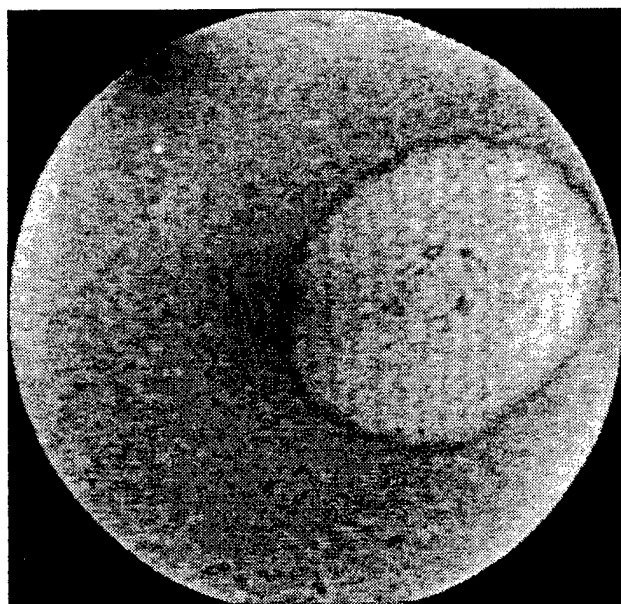
step structures and the rest featureless with uniform gray contrast. On the stepped region, initial nucleation at the step edges occurred with growth spreading across the terraces. After about 1 hour, graininess developed in the ordered region as well as in the disordered region with the appearance of some bright spots. Finally, when the growth was extended to 200 minutes and beyond, the LEEM image in Fig. 4 shows very grainy features in the originally ordered region and aggregates of crystals in the disordered region.

The LEED patterns corresponding to the GaN growth by SSJ is shown in Fig. 5. With increasing deposition time, weak and diffuse arced diffraction spots developed with strong secondary electron background as shown in the frame at 84 minutes and 19.7 eV electron energy. The arced features merged into single spots and streaky diffraction features developed when the energy was reduced to 7.0 eV (84 min), accompanied by a reduction of secondary electron background. The movement and change of the diffraction features with energy indicate that they were originated from faceted and azimuthally poorly aligned crystals. The LEED patterns at longer deposition times show the arc features sharpening at 19.7 eV and the spots becoming clearer and more intense at 7.0 eV, indicating well-developed faceted crystals of GaN. The LEED patterns obtained for the GaN growth with the RF plasma source are very similar to those shown in Fig. 5.

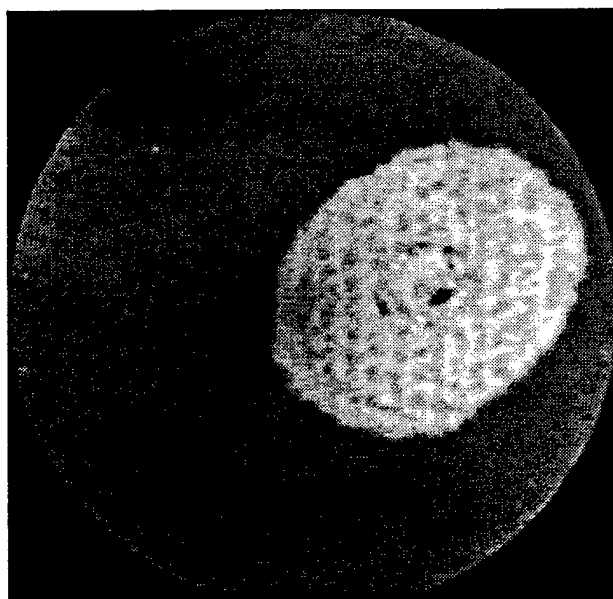
Both the LEEM and LEED results confirm the growth of faceted GaN crystals with the SSJ source. LEED analysis shows that growth of the (0001) surface is almost absent with the dominant facets being  $\{10\bar{1}1\}$  and possibly also  $\{10\bar{1}2\}$ . The growth on the well-ordered region is similar to deposition conducted with the N-atom RF plasma source although basal plane growth is more in evidence Fig. 3. The surfaces of both grown film is rough on a submicron scale. Adsorption of oxygen could be a cause for the faceting behavior, but further experiments with gases introduced via purifiers are needed to confirm this conjecture. Gas analysis in the LEEM chamber shows that the  $O_2:N_2$  ratio is  $\sim 5 \times 10^{-6}$  in the SSJ experiments. In the RF plasma source experiments, this ratio is higher at  $\sim 2 \times 10^{-5}$ . Post mortem Auger depth profiling shows an oxygen signal throughout the grown film, which could be attributed to oxygen on the side facets of the columnar shaped crystals of GaN.

#### D. Conclusions

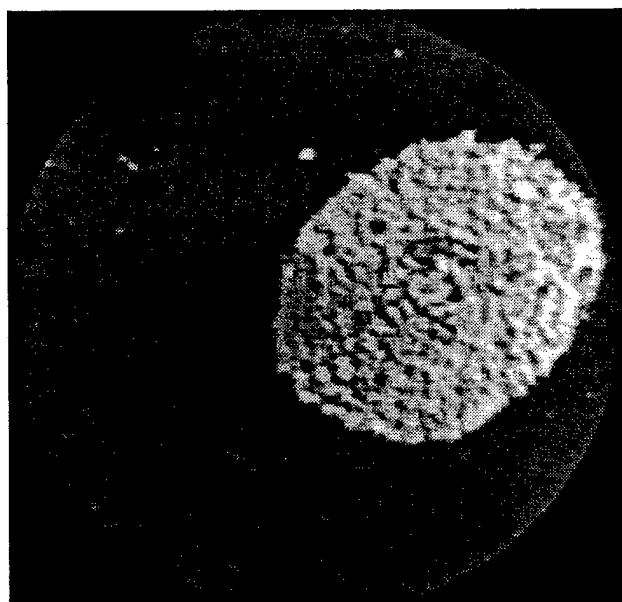
Our *in situ* real-time observations of GaN growth on 6H-SiC(0001) substrates with LEEM/LEED indicate that the grown films consist mainly of three-dimensional crystallites. They probably have a columnar structure [13] with predominantly  $\{10\bar{1}1\}$  and  $\{10\bar{1}2\}$  facets on the top surface of the film. The homogeneity of the SiC substrate surface needs to be improved to ensure uniformity in the LEEM observations of GaN growth. Experiments involving expanded growth parameters as well as GaN homoepitaxy are under way.



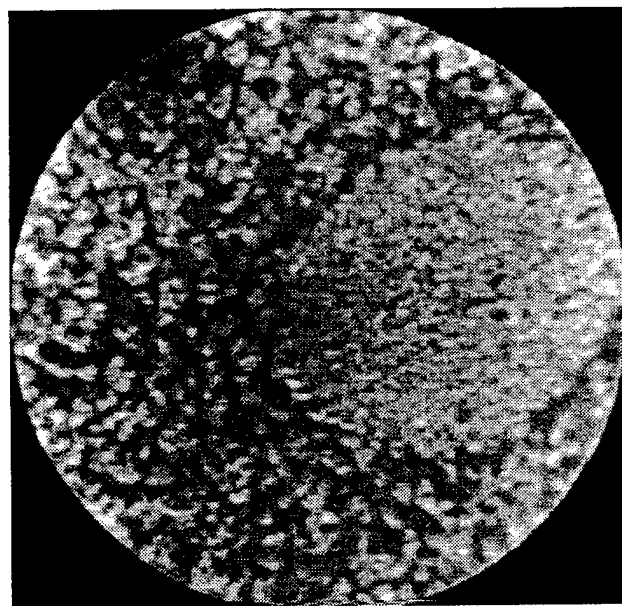
Initial surface



7min

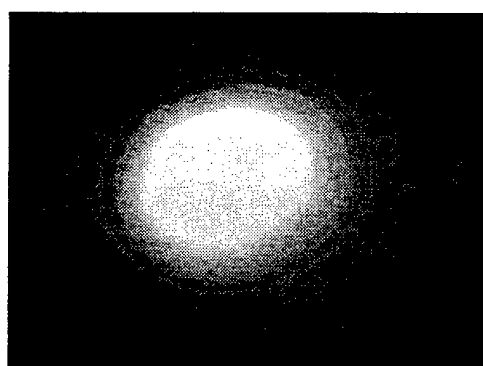


64 min

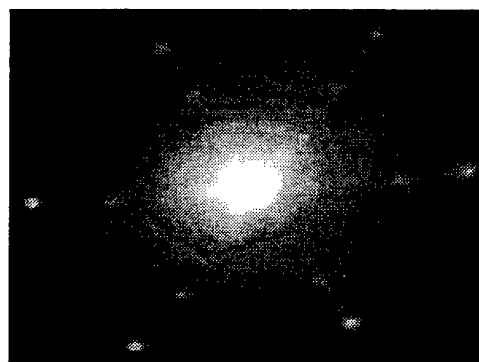


200 min

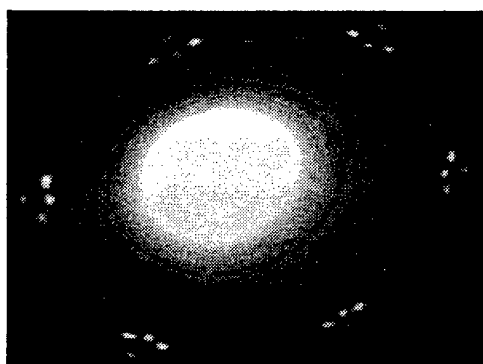
Figure 4. LEEM video images showing GaN growth with the SSJ source. Field of view  $4.8\ \mu\text{m}$ , electron energy  $7.0\ \text{eV}$ .



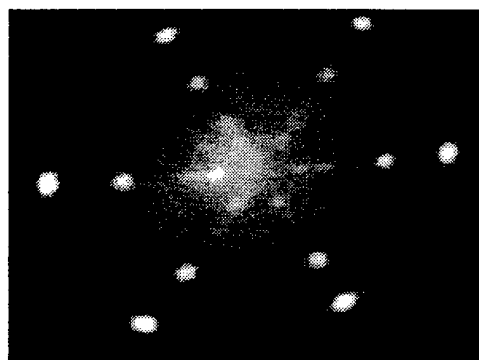
84 min, 19.7 eV



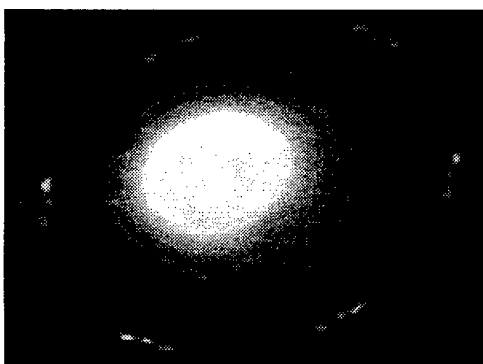
84 min, 7.0 eV



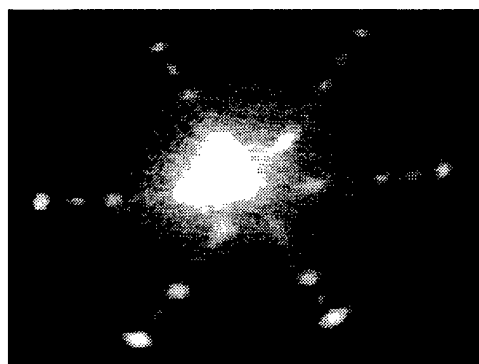
145 min, 19.7 eV



145 min, 7.0 eV



230 min, 19.7 eV



230 min, 7.0 eV

Figure 5. LEED patterns taken at two different energies, 19.7 eV and 7.0 eV, during GaN growth with the SSJ source.



## E. Acknowledgments

This work was supported by the Office of Naval Research grant N00014-95-1-0122; the National Science Foundation MRSEC grant DMR-9632635; and the Deutsche Forschungsgemeinschaft.

## F. References

1. S. Nakamura, T. Mukai and M. Seno, Jpn. J. Appl. Phys. **30**, L 1998 (1991).
2. S. Nakamura, J. Cryst. Growth **170**, 11 (1997).
3. S. Strite and H. Morkoc, J. Vac. Sci. Technol. **B10**, 1237 (1991).
4. H. Morkoc, S. Strite, G.B. Gao, M.E. Lin, B. Sverdlov and M. Burns, J. Appl. Phys. **76** (1994) 1363.
5. S.T. Ceyer, Science **249**, 82 (1990).
6. S.T. Ceyer, Langmuir **6**, 82 (1990).
7. V. M. Torres, M. Meloni and R. B. Doak, (unpublished)
8. V. M. Torres, M. Stevens, J. L. Edwards, D. J. Smith, R. B. Doak and I.S.T. Tsong, Appl. Phys. Lett. (in press).
9. E. Bauer, Rep. Prog. Phys. **57**, 895 (1994).
10. J. Nogami, S. I. Park and C. F. Quate, Surf. Sci. **203**, L631 (1988).
11. E. Bauer, Y. Wei, T. Müller, A. Pavlovskaya and I.S.T. Tsong, Phys. Rev. **B 51**, 17891 (1995).
12. R. B. Doak, in: *Atomic and Molecular Beam Methods*, Vol. 2, Ed. G. Scoles (Oxford Univ. Press, 1988) Ch. 14.
13. F. A. Ponce, MRS Bulletin **22**, 51 (1997).

## **IV. Effects of Energy and Angle of Incidence on AlN and GaN Epitaxial Growth using Helium Supersonic Beams Seeded with NH<sub>3</sub>**

### **A. Introduction**

The nitride family of AlN, GaN and InN thin films have shown to be strong candidates for electronic and optoelectronic applications. With direct band gaps of 6.2 eV, 3.4 eV and 1.9 eV for AlN, GaN and InN respectively, solid solutions based on these materials provide for band gap modifications suitable for applications ranging from the red to the deep UV region of the spectrum [1]. Due to the high bond strength between N and H in NH<sub>3</sub>, the growth of III-V nitrides requires high substrate temperatures unless some other form of activation is present. Supersonic molecular beam epitaxy (SMBE) has been shown to enhance the surface decomposition of silane and methane [2,3] because of the possibility of tuning the kinetic energy of these species to deform and cleave the bonds upon impact with the substrate. In addition the tuning of the energy spread is possible with SMBE. This is important in order to experimentally determine the chemisorption barriers for the systems being studied as well as to provide species with high sticking coefficients at high enough intensities. SMBE is therefore a useful technique for the low-temperature growth of single-crystalline GaN films at suitable growth rates using NH<sub>3</sub>. A review of supersonic molecular beams can be found in Scoles [4].

A UHV deposition chamber has been interfaced with the supersonic beam source chamber. The deposition chamber is being used for deposition of AlN and GaN on 6H-SiC(0001) substrates using the seeded beams.

### **B. Deposition Chamber Description**

The deposition chamber used for the current deposition experiments is the same deposition chamber used for previous MBE work at ASU [Dec. 96 Progress Report]. A series of modifications have been made to the chamber in order to decrease the power requirements for the Ga and Al evaporators, increase the sample throughput and vary the angle of incidence of the seeded beam.

A schematic of the Al evaporator is shown in Fig. 1. The evaporator was approximately 5" away from the sample and was heated with a tungsten filament. A tantalum shield was placed around the filament and the crucible such that only the outer surface of the crucible was heated and the inner surface of the crucible was exposed toward the substrate. The crucible was supported at the top by a Ta strip in order to cool the upper part of the crucible to prevent Al from overflowing during evaporation. The evaporator was tested and the flux rates achieved were similar to those obtained previously even though 30% less power was needed. This reduction in power also decreased the amount of degassing in the chamber. A second evaporator for Ga was also built using a similar design.

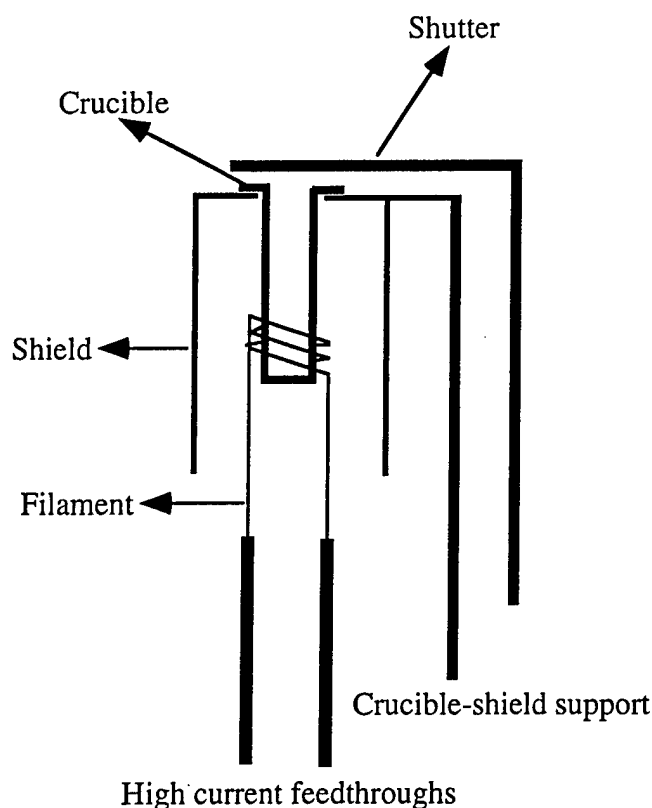


Figure 1. Al evaporator schematic.

A new sample carousel capable of holding three samples was built. This assembly enabled an increase in the sample throughput. The samples were heated by passing a DC current through them. A laser was used to insure that the samples were aligned with respect to the seeded beam. The carousel was tested thoroughly and worked in a very reproducible fashion. By replacing a minimum number of parts on the carousel, the angle of incidence could be changed from  $90^\circ$  to  $45^\circ$  and  $15^\circ$ .

AlN was grown in the system described above. The samples were analyzed by Rutherford backscattering spectroscopy and Auger electron spectroscopy and were found to contain carbon. At the present time, attempts are being made to eliminate the contamination problem.

#### C. Conclusion

The seeded beam source chamber was interfaced with a UHV deposition chamber. The deposition chamber housed two evaporators and a sample carousel capable of holding three samples. The whole system was thoroughly tested. AlN films were grown with this system.

#### D. Future Work

In the next three month period, work will begin on depositing AlN and GaN epitaxial layers on 6H-SiC(0001) using our seeded beam. Study will be made of the effects of increasing the  $\text{NH}_3$  kinetic energy and varying the angle of incidence.

## E. References

1. S. Strite and H. Morkoc, J. Vac. Sci. Technol. **B10**, 1237 (1992).
2. M. E. Jones, L. Q. Xia, N. Maity, J. R. Engstrom, Chem. Phys. Lett. **229**, 401 (1994).
3. S. T. Ceyer, J. D. Beckerle, M. B. Lee, S. L. Tang, Q. Y. Yang, M. A. Hines, J. Vac. Sci. Technol. A **5**, 501 (1987).
4. D. R. Miller, *Atomic and Molecular Beam Methods*, Ch. 2, Ed. G. Scoles, Oxford University Press (1988)

## V. Homoepitaxial Growth of Stoichiometric GaN Films using an Ammonia-seeded Supersonic Beam

### A. Introduction

Gallium nitride is a wide band gap semiconductor ( $E_g=3.4$  eV) with many potential optoelectronics and high-temperature, high-frequency, microelectronics applications. Gallium nitride forms a continuous range of solid solutions with AlN (6.28 eV) and InN (1.95 eV), permitting the fabrication, via bandgap engineering, of laser diodes with tunable emission frequencies from covering the visible and UV regions. State-of-the-art GaN films ( $\leq 10^8$  defects per  $\text{cm}^2$ ) have been used to fabricate blue light emitting diodes (LEDs) and laser diodes.

Heteroepitaxial growth of high-quality monocrystalline GaN films has been problematic due to the lack of a suitable lattice-matched substrate and the thermodynamic instability of GaN under high-temperature growth conditions. Sapphire, the most common substrate, exhibits a 14% lattice mismatch at the GaN(0001)/sapphire(0001) interface; moreover, the thermal expansion coefficient of sapphire is 25% greater than that of GaN. Only by employing a low-temperature AlN or GaN buffer layer can one obtain monocrystalline GaN films on sapphire with defect densities in the  $10^8$ - $10^9$   $\text{cm}^{-2}$  range.

Substrate temperatures in excess of  $1000^\circ\text{C}$  are employed for growth of monocrystalline GaN films by halide or metal-organic CVD (MOCVD) using  $\text{NH}_3$ . In MOCVD, substrate thermal energy is used to overcome activation barriers for precursor decomposition and adatom surface migration (lateral diffusion); however, GaN decomposition above  $620^\circ\text{C}$  *in vacuo* necessitates the use of large V/III flux ratios [1]. Plasma-assisted processes have been utilized to lower the GaN growth temperature to approximately  $700^\circ\text{C}$ , but ion-induced damage and oxygen contamination are often observed.

The use of energetic neutral beams of precursor molecules is an alternative approach to the epitaxial growth of GaN films at lower substrate temperatures. In selected energy epitaxy (SEE), heavy reactant molecules are seeded in a supersonic expansion of light molecules and thereby accelerated to hyperthermal energies. The precursor molecules attain kinetic energies on the order of 1-2 eV which can provide the necessary energy for activated surface processes, such as dissociative chemisorption and adatom migration. Hence, in prospect, monocrystalline GaN films may be grown at lower substrate temperatures by SEE than by conventional MOCVD [2]. Moreover, energetic neutral beams with narrow energy distributions are ideal tools for fundamental studies of wide bandgap semiconductor growth using *in situ* low-energy electron microscopy (LEEM) and other techniques.

To demonstrate the potential advantages of SEE, homoepitaxial growth of GaN was investigated obviating the substrate lattice-mismatch issue and allowing us to better isolate the effects of precursor kinetic energy on growth kinetics and film morphology. Results of GaN

homoepitaxial growth using TEG-seeded and  $\text{NH}_3$ -seeded supersonic molecular beams were described in the previous report (June 1997). In this report, detailed results of GaN homoepitaxial growth using a  $\text{NH}_3$ -seeded supersonic beam and effusive Ga source are presented, and the effects of substrate temperature and Ga flux on growth rate and morphology are elucidated.

## B. Experimental Procedure

*SEED/XPS Deposition System.* The SEED/XPS multi-chamber system described in previous reports (June 1996, Dec. 1996) was used for homoepitaxial growth of GaN. The orifice used in the  $\text{NH}_3$  nozzle was 150  $\mu\text{m}$ . A conical skimmer used for extracting the  $\text{NH}_3$  beam from the supersonic free jet has an opening of 1 mm in diameter, a base of 20 mm in diameter, an included angle of  $25^\circ$  at the opening and of  $70^\circ$  at the base, and a height of 17 mm. The collimation aperture of  $5 \times 5 \text{ mm}^2$  is located downstream between the 2nd differential pumping stage and the growth chamber. The molecular beam is directed to the substrate with an incident angle of  $6^\circ$  with respect to the surface normal. The deposition area on the vertical substrate is  $15 \times 15 \text{ mm}^2$ .

*Substrate Preparation/Cleaning.* The substrates were 2- $\mu\text{m}$  thick GaN films grown by MOCVD on on-axis 6H-SiC employing a 0.1- $\mu\text{m}$  thick AlN buffer layer. The substrates were provided by M. Bremser and O. Nam of Prof. Davis's group and used as received. Ag paste was used to provide good thermal contact between the Mo sample holder and the GaN/AlN/6H-SiC substrate; two Mo pins were used to hold the substrate in place. The Mo holder was placed on a hot plate to dry the Ag paste for 5 min at  $80^\circ\text{C}$ . Subsequently, it was introduced via the load-lock chamber and transferred *in vacuo* into the growth chamber. Each sample was heated slowly to  $400^\circ\text{C}$  under an  $\text{NH}_3$  flux for outgassing. Prior to the growth, the GaN substrate was cleaned *in situ* by  $\text{NH}_3$  beam exposure at  $730^\circ\text{C}$  for 30 min, unless otherwise noted. After *in situ* cleaning the substrate temperature was lowered to  $200^\circ\text{C}$  under an  $\text{NH}_3$  flux. The GaN substrate was examined by RHEED before and after *in situ* cleaning to ensure that the surface was clean prior to growth. *In situ* Ga cleaning of GaN was also examined. The substrate was coated by Ga deposition at room temperature for 2 min with the Ga K-cell heated to  $950^\circ\text{C}$ . The substrate was then heated to  $730^\circ\text{C}$  *in vacuo* for 5-15 min to evaporate the Ga.

*Homoepitaxial Growth Using Supersonic An  $\text{NH}_3$  Beam and Ga Effusion Cell.* A hot-lip Ga Knudsen cell (K-cell) described in the previous report (June 1997) was used for the homoepitaxial growth of GaN. Films were grown using the Ga cell and a  $\text{NH}_3$ -seeded supersonic molecular beam. Growth was initiated by opening the K-cell shutter after both the Ga crucible and the substrate were at the desired temperatures. Growth runs lasted for two hours, unless otherwise noted. The  $\text{NH}_3$  nozzle was heated to  $200^\circ\text{C}$  and the stagnation

pressure was in the 745-755 Torr range for typical experiments, which employed a  $\text{NH}_3$  flow rate of 60 sccm and a He flow rate of 200 sccm. GaN growth experiments were done in the substrate temperature range of 620-730°C. The Ga K-cell temperatures ranged from 900°C to 1000°C. Growth rates were determined using SEM cross-sectional images.

**XPS Analysis.** The UHV surface analysis chamber is equipped with a PHI 3057 XPS system comprising a 10-360 spherical capacitor analyzer (SCA), Omni Focus III fixed-aperture lens, 16-element multichannel detector, and 257 DR11 PC interface card. A PHI 1248 dual-anode (Al/Mg) X-ray source is used. The sample is mounted on a tilt stage which is attached to a precision xyz-rotary manipulator (Thermionics). The analysis chamber is pumped by a Perkin-Elmer TNBX ion pump/TSP combination and has a base pressure of  $8 \times 10^{-11}$  Torr. After growth, samples were transferred to the XPS chamber through vacuum transfer lines. XPS spectra were taken with both Mg and Al anodes to isolate N(1s), O(1s), C(1s) and Ga(2p<sub>3/2</sub>) photoelectron peaks from other interfering signals.

**RHEED Analysis.** *In situ* reflection high-energy electron diffraction (RHEED) measurements were made using a Fisons LEG 110 15-kV electron gun and 100-mm Al-coated phosphor screen. RHEED patterns of the GaN substrate before and after the *in situ* cleaning, and after GaN growth were taken at 15kV.

**SEM Analysis.** Scanning electron microscope images of GaN films were obtained using a JEOL 6400FE SEM with a 5-kV cold field emission electron gun. Both surface and cross sectional images were taken.

### C. Results and Discussion

***In situ* Substrate Cleaning.** Table I shows the surface carbon and oxygen concentrations obtained by XPS of MOCVD-grown GaN substrates before and after *in situ* cleaning.

A sample (Run 1) coated with Ga and then heated *in vacuo* at 730°C for 5 min showed a substantial reduction in carbon and oxygen contamination. A second sample (Run 2) was coated with Ga, first heated *in vacuo* at 730°C for 15 min and then heated at 730°C under an  $\text{NH}_3$  flux for 15 min gave a better result. When the heating time was increased from 5 to 15 min after Ga coating the substrate, the oxygen content was nearly the same, whereas the carbon content increased slightly. The carbon concentration typically increased to a maximum and then decreased with continued heating *in vacuo* or under a  $\text{NH}_3$  flux (Run 3). This carbon contamination was been traced to the Ag paste used between the substrate and the Mo sample holder, as discussed in a previous report (June 1997). A streaky RHEED pattern with Kikuchi lines, that was clearer than the pattern before *in situ* cleaning, was observed after Ga and/or  $\text{NH}_3$  cleaning. Among these cleaning techniques, Ga cleaning for 15 min followed by the  $\text{NH}_3$  cleaning for 15 min gives the lowest carbon and oxygen concentrations.

Table I. Surface Carbon and Oxygen Concentrations for Different GaN *in situ* Cleaning Conditions

Run	Conditions	C %	O %
1	GaN substrate without cleaning	14	11
	Ga coated, heated at 730°C for 5 min	8	4
2	GaN substrate without cleaning	12	11
	Ga coated, heated at 730°C for 15 min	11	4
	NH <sub>3</sub> cleaning at 730°C for 15 min	5	3
3	GaN substrate without cleaning	12	10
	Heated <i>in vacuo</i> at 800°C for 15 min	22	7
	NH <sub>3</sub> cleaning at 800°C for 15 min	7	3

*Homoepitaxial Growth Using Supersonic NH<sub>3</sub> Beam and Ga K-cell.* Growth runs were conducted at substrate temperatures varying from 620°C to 730°C with Ga K-cell temperatures of 900°C to 1000°C. The characteristics of selected films grown at different substrate temperatures and Ga K-cell temperatures are summarized in Table II. All films grown in the stated ranges of substrate temperature and Ga K-cell temperature were stoichiometric, excluding the film coated with Ga droplets. The GaN growth rate is nearly independent of substrate temperature, but increases slightly as the Ga flux from the effusion cell increases.

Table II. Characteristics of Selected Homoepitaxial GaN Films

Film	Temp (°C) Substrate	Temp (°C) Ga K-Cell	Growth Rate (nm/hr)	Ga/N	Growth Morphology
71897	620	900	70	1.00	3D; Sharp pyramids
81497	660	950	70	1.07	3D; Rounded pyramids
82297	660	960	92	1.51	2D; Covered in Ga droplets
82597	730	900	75	1.03	3D; Rounded pyramids
82697	730	950	80	1.01	3D; Coalesced islands
82797	730	960	90	1.04	2D; Smooth with growth pits



Figures 1-5 are SEM images illustrating the various growth morphologies observed. As the Ga flux from the K-cell is increased at 730°C substrate temperature, the film morphology changes from rounded pyramidal islands (Fig. 2) to coalesced islands (Fig. 3) to a smooth surface with growth pits (Fig. 4). This indicated that a minimum Ga flux was needed for a 2D homoepitaxial growth; however, further increase in the Ga flux resulted in the formation of Ga droplets on the film surface. Thus, we concluded that there existed a narrow range of Ga flux, corresponding to slightly Ga-rich growth conditions, in which 2D homoepitaxial growth was possible.

Film morphology was also dependent on substrate temperature. With an increase in the substrate temperature at constant Ga flux the islands became smoother and less pyramidal (compare Fig. 1 and Fig. 2). RHEED data confirms the change in film morphology. As the growth temperature increased from 660°C to 730°C for a constant Ga K-cell temperature, the RHEED pattern changed from spots to a mixture of spots and streaks.

Figures 4 and 5 show a smooth homoepitaxial film. The cross sectional view (Fig. 5) indicates that the SEE-grown GaN is 0.18  $\mu\text{m}$  thick. The MOCVD GaN substrate consists of two layers of lightly and heavily doped GaN. The AlN-buffered SiC substrate is the dark layer beneath the GaN.

The smooth films exhibit some small holes and hexagonal pits. Some of these defects were the result of micropipes in the MOVPE GaN substrate. SEM images of the substrate were taken and show similar holes on the surface extending to the SiC substrate. An example of a growth pit in the homoepitaxial layer can be seen in the lower right corner of Fig. 4. A possible cause for these growth pits is carbon and oxygen contamination. Typically, the carbon concentration at the GaN film surface is 6 to 14 %, and the oxygen concentration is 5 to 9 %.

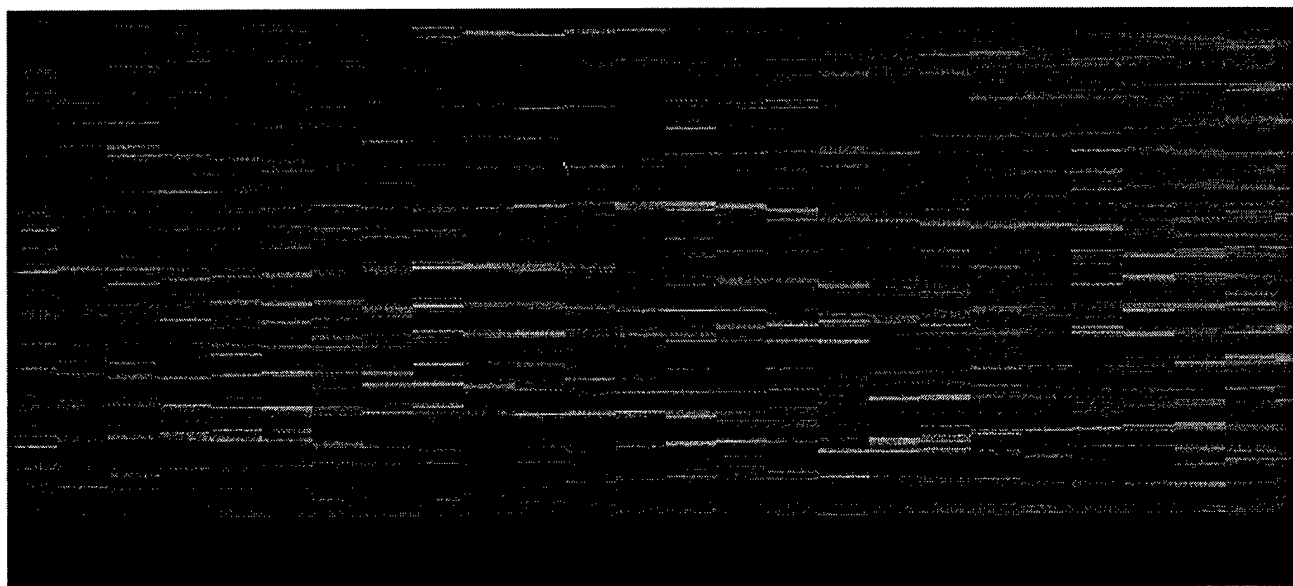


Figure 1. GaN grown at 620°C, Ga K-Cell at 900°C, Film 71897.

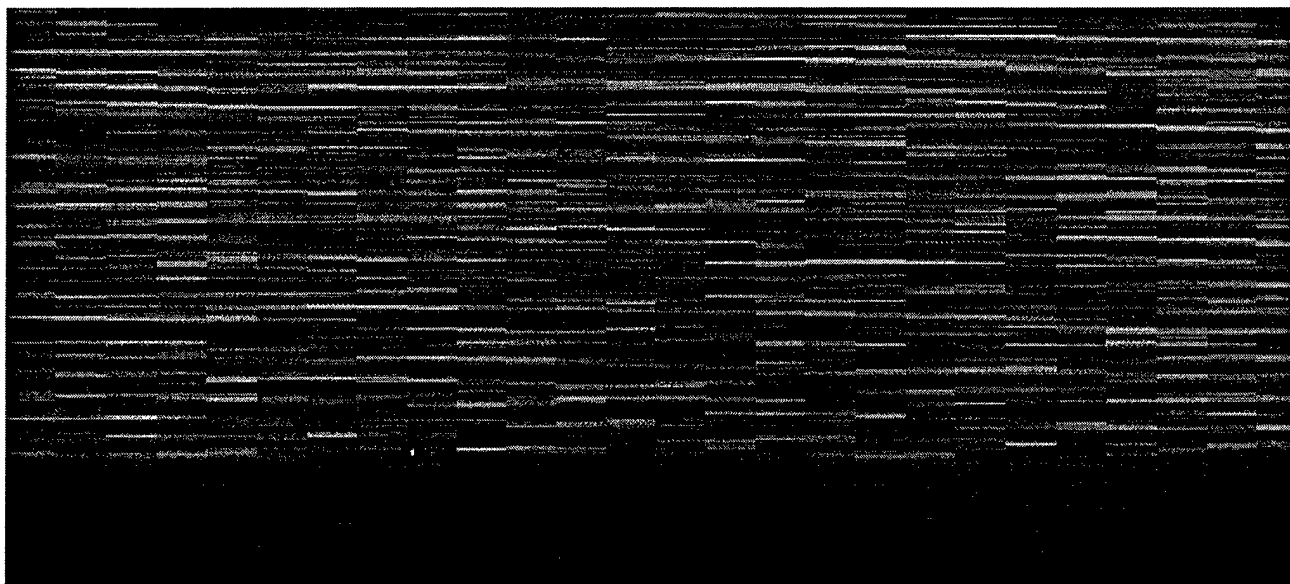


Figure 2. GaN grown at 730°C, Ga K-Cell at 900°C, film 82597.

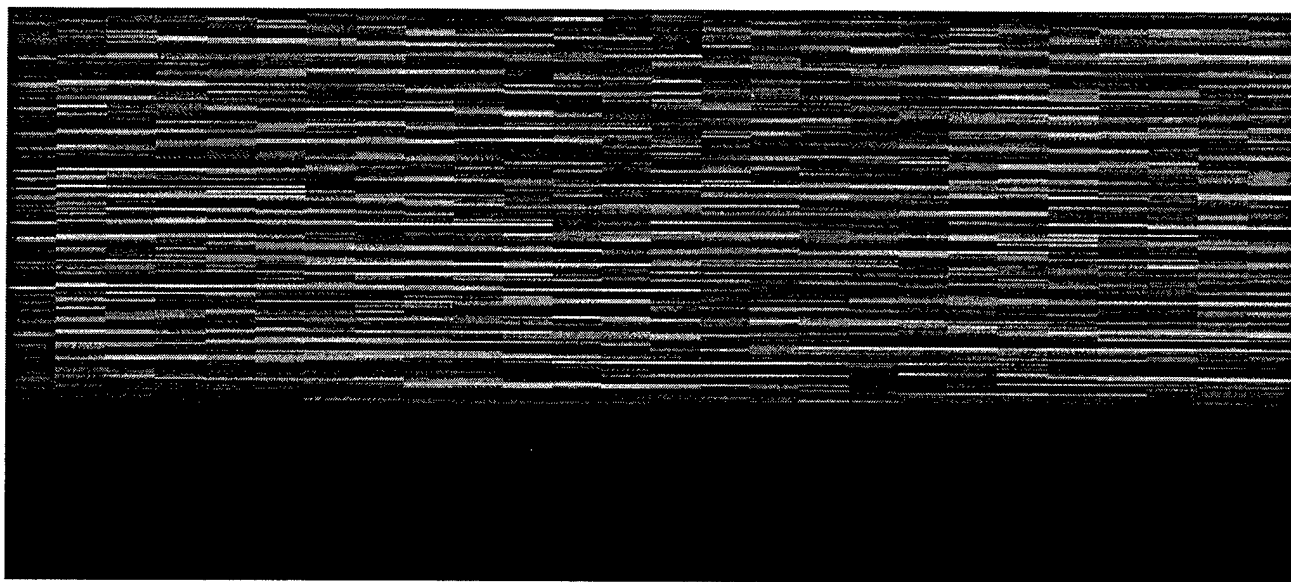


Figure 3. GaN grown at 730°C, Ga K-Cell at 950°C, film 82697.

#### D. Conclusions

Homoepitaxial growth of smooth, stoichiometric GaN films using a Ga K-cell and  $\text{NH}_3$ -seeded supersonic beam was achieved. The smoothest films were achieved at a growth temperature of 730°C and a Ga K-Cell temperature of 960°C. Without sufficient Ga flux and substrate thermal energy, three-dimensional growth was observed. The achievement of smooth film growth using a Ga effusion cell provides a starting point for future studies of two-dimensional homoepitaxial growth using dual  $\text{NH}_3$ - and TEG-seeded supersonic beams.

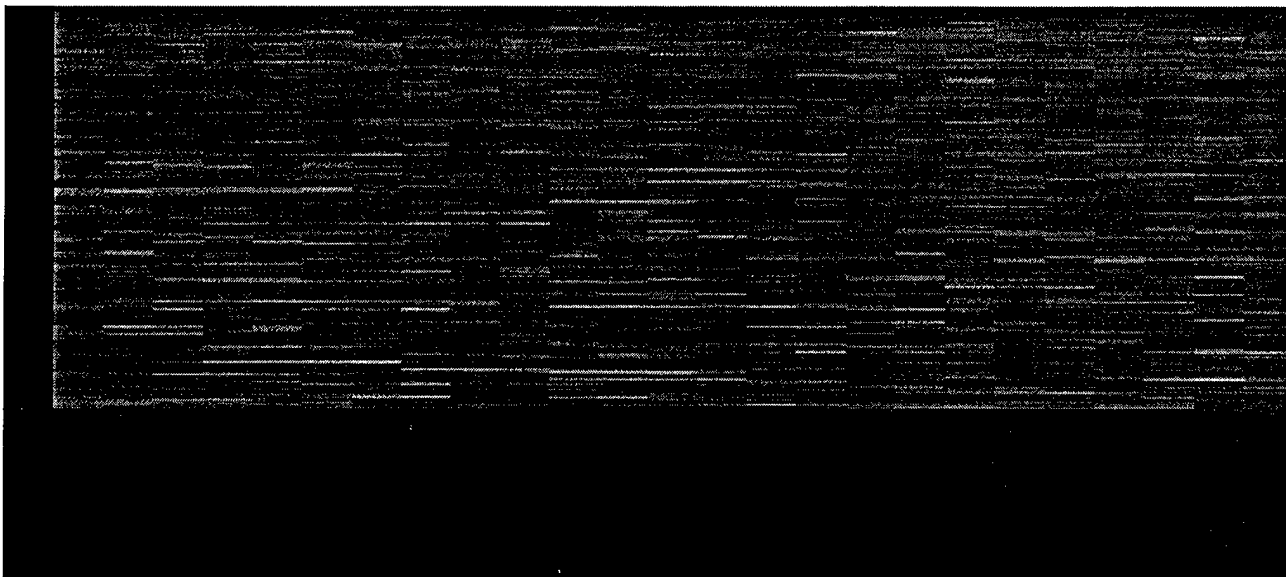


Figure 4. GaN grown at 730°C, Ga K-Cell at 960°C, film 82797.

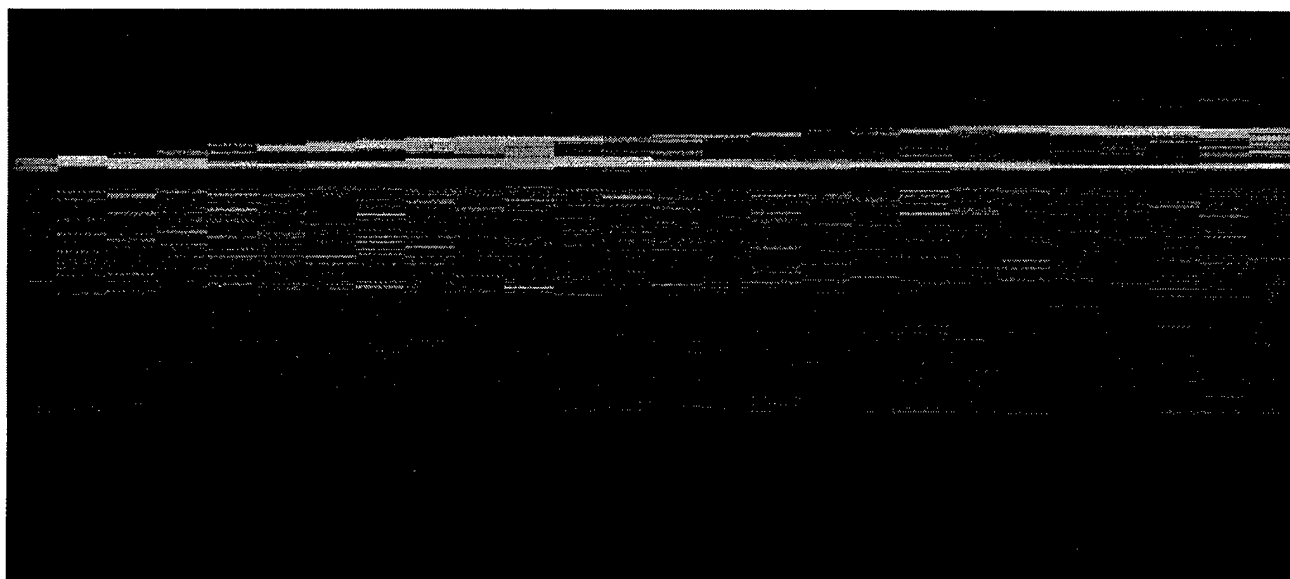


Figure 5. GaN grown at 730°C, Ga K-Cell at 960°C, cross section of film 82797.

#### E. Future Plans

A more detailed investigation of GaN homoepitaxial growth using dual  $\text{NH}_3$ - and TEG-seeded supersonic beams will be made to elucidate the relationships between film quality and precursor kinetic energies, as tuned by seeded supersonic beams. Results from the growth of smooth films using the Ga K-cell will be used to estimate the Ga flux needed to grow smooth films using a TEG-seeded supersonic beam.

Time of flight (TOF) velocity measurements will be made in order to establish the kinetic energy distributions of the seeded supersonic molecular beams.

A new gas line for generating TEA (triethylaluminum)-seeded supersonic beam will be installed and used to grow an AlN buffer layers on 6H-SiC substrates.

A radio-frequency discharge nozzle/nitrogen atom source [3,4] will be constructed and installed in the system. This source will produce a supersonic beam of atomic nitrogen and will be used in conjunction with the TEG supersonic source and the Ga effusion cell for GaN growth.

Real-time RHEED intensity measurements will be used to investigate the growth mode of GaN epilayers. In the short term, a photomultiplier tube will be mounted in front of the RHEED screen to monitor the intensity of the specular beam. Long-term plans include a CCD camera-based RHEED data acquisition system.

#### F. References

1. S. Nakamura, Japan. J. Appl. Phys. **30**, L1705 (1991).
2. M. R. Lorenz and B. B. Binkowski, J. Electrochem Soc. **109**, 24 (1962).
3. C. B. Mullins, Appl. Phys. Lett. **68**, 3314 (1996).
4. J. E. Pollard, Rev. Sci. Instrum. **63**, 1771 (1992).

## VI. Deposition of GaN Thin Films by Dual Low-energy Ion Beams

N. Freed<sup>1</sup>, C. Linsmeier<sup>2</sup>, and I.S.T. Tsong<sup>1\*</sup>

<sup>1</sup>Department of Physics and Astronomy, Arizona State University, Tempe, AZ 85287-1504, USA

<sup>2</sup>Max-Planck-Institute für Plasmaphysik, D-85748 Garching, Germany

\* To whom correspondence should be addressed. E-mail: ig.tsong@asu.edu

We have designed and constructed a dual Colutron ion-beam system for the purpose of deposition of wide bandgap semiconductor thin films. By outfitting the two Colutron units with deceleration lenses, we were able to produce mass-analyzed  $\text{Ga}^+$ ,  $\text{N}_2^+$  and  $\text{N}^+$  ions at  $\sim 20$  eV with a small energy spread of  $\sim 1$  eV at FWHM. The  $\text{N}_2^+$  and  $\text{N}^+$  ion beams were used to perform nitridation of Si(100) surfaces. Subsequent SIMS depth profiles indicated the presence of nitride layers on the Si(100) substrates. Codeposition of Ga and N on Si(111) and Si(100) substrates was conducted with the  $\text{Ga}^+$  and  $\text{N}_2^+$  ion beams. SIMS depth profiles showed the presence of both Ga and N on the Si substrate surfaces suggesting the formation of a GaN layer.

## A. Introduction

Tremendous interests have been shown in the past few years on the Group III nitrides GaN, AlN, InN, and their alloys in the form of epitaxial films because they can be used to fabricate short-wavelength light emitting diodes (LED's) and laser diodes (LD's) [1,2], as well as high-power, high frequency and high-temperature electronic devices [3]. In spite of these successful applications, optimization of the Group III nitride materials is still in progress in terms of reduction of defect densities and impurities, and lowering of substrate temperatures during deposition. In this report, we describe a new approach to synthesize the wide bandgap (3.4 eV) compound semiconductor GaN thin films by codepositing low-energy  $\text{Ga}^+$  and  $\text{N}_2^+$  ions from a dual Colutron ion-beam system.

The rationale of using low-energy monoenergetic ion beams for deposition is to locate an energy window in which the ion-energy is high enough to overcome the activation barrier such that the reaction of the Ga and N species can proceed easily on the substrate surface, while at the same time low enough not to cause radiation damage in the deposited film. Additionally, at this energy window, the deposited species have sufficient translational energy to migrate to preferred sites such as step edges on the substrate surface, thereby enhancing epitaxial growth even at low substrate temperatures.

Homoeptaxy of Si and of Ge by direct ion-beam deposition have been reported recently [4-7]. Heteroeptaxy of Ge on Si(100) and oxidation of Si(100) have also been described in these reports. Ion energies of  $\sim 20$  eV appear to provide the best results and epitaxial films were obtained at substrate temperatures as low as  $\sim 200^\circ\text{C}$ . Brice *et al.* [8] have conducted calculations of the number and partitioning of displacements of surface and bulk atoms by low-energy ions incident on a solid to explain the above observations. As far as we know, there has never been any attempt to use low-energy ion beams to codeposit a compound semiconductor or an alloy film. The present report is the first such attempt.

## B. Experimental

The dual ion-beam deposition unit is depicted in Fig. 1. The two Colutron ion sources [9] are each equipped with a  $\mathbf{E} \times \mathbf{B}$  velocity filter (or Wien Filter) to select the mass of the desired ions. By outfitting the Colutron units with electrostatic deceleration lenses, the ions can be slowed down to the 10 eV range from an initial energy of  $\sim 1$  keV. In order to maintain ground potential at the target sample, the entire Colutron unit, i.e. ion source, acceleration and focusing system, deflection plates, and velocity filter, are floating at a negative potential of  $\sim 1\text{kV}$ . The deposition system is equipped with RHEED to monitor in situ film growth, a 4-grid retarding field analyzer to conduct LEED and AES to analyze surface structure and composition of the deposited film, an electrostatic energy analyzer to determine the energy distribution of the ions, and a movable Faraday cup to measure the ion beam current and its spatial distribution.

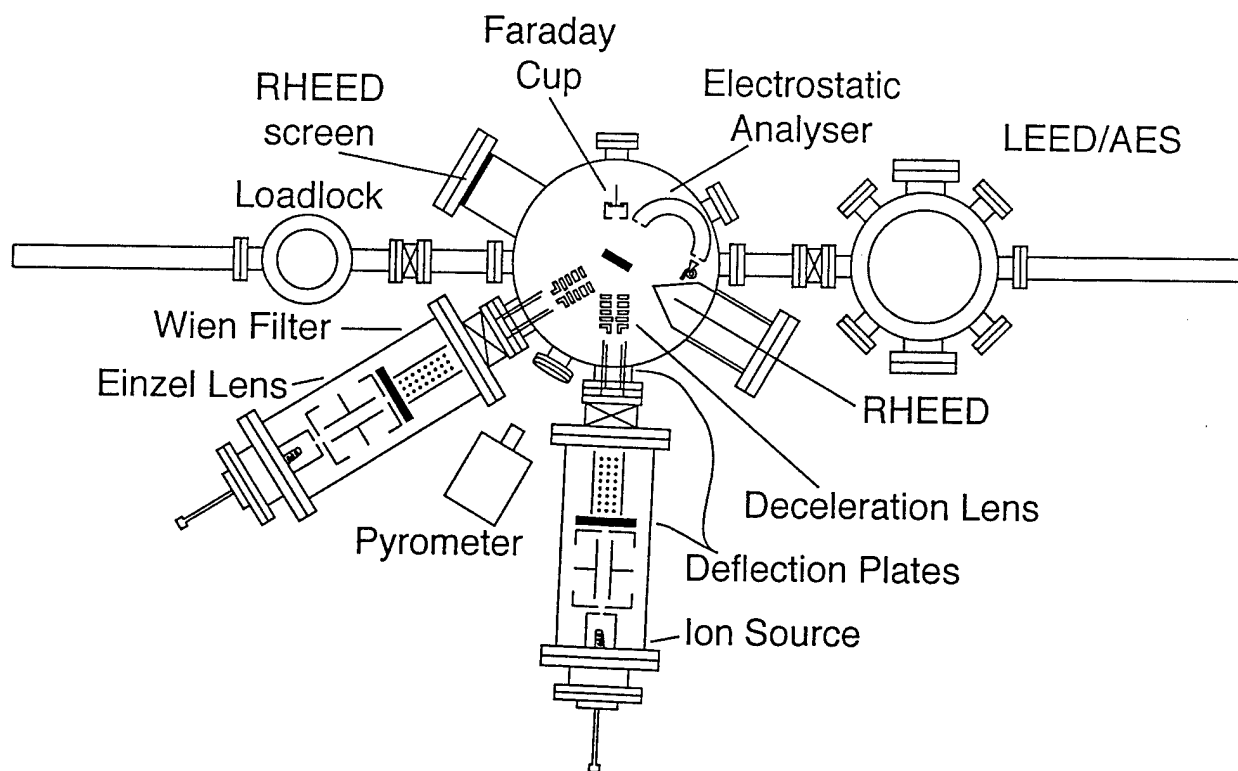


Figure 1. Schematic diagram of the dual Colutron ion-beam deposition system.

After the completion of the dual Colutron ion-beam deposition system, the energy distribution of the  $\text{Ga}^+$ ,  $\text{N}_2^+$ , and  $\text{N}^+$  ions were measured. Nitridation of a  $\text{Si}(100)$  surface using  $\text{N}_2^+$  and  $\text{N}^+$  ions at  $\sim 40$  eV was carried out with one of the two Colutron sources. SIMS depth profiles of the nitrided surfaces were taken using a Cameca IMS-3f to confirm the presence of nitride layers on the substrate surfaces. This was followed by experiments where codeposition of  $\text{Ga}^+$  and  $\text{N}_2^+$  ions at  $\sim 20$  eV on  $\text{Si}(111)$  and  $(100)$  substrates took place. SIMS depth profiles were taken to check the existence of GaN layers on the substrates. All the Si substrates were etched by HF to remove the native oxide prior to installation in the deposition chamber.

Because of the deceleration process, the ion beam currents were greatly reduced and they were generally operated in the 10-50 nA range with beam spot sizes around 5 mm in diameter. This gives an ion flux of  $\sim 1 \times 10^{12} \text{ cm}^{-2} \text{ s}^{-1}$  which means that it takes anywhere from 15 to 30 minutes to achieve a full monolayer coverage on a Si substrate. The deposition experiments typically took several hours for each run. At this preliminary stage of evaluating our dual ion-beam deposition system, we did not bake the system to achieve UHV. The base pressure in the deposition chamber was  $\sim 3 \times 10^{-9}$  Torr, rising to  $\sim 1 \times 10^{-7}$  Torr during deposition.

### C. Results and Discussion

The energy distributions of the  $N_2^+$ ,  $N^+$  and  $Ga^+$  ions at  $\sim 20$  eV are shown in Figs. 2, 3 and 4 respectively. The distributions indicate that the ions are essentially near-monoenergetic, with FWHM at  $\sim 1$  eV. The most important feature is the absence of high energy tails in these distributions, which means damage to the films will be kept to a minimum.

The nitridation of the Si(100) surface by low-energy  $N_2^+$  and  $N^+$  ions is shown in the SIMS depth profiles in Fig. 5. The relative counts of  $CsSi^+/Cs^+$  and  $CsN^+/Cs^+$  are plotted as a function of depth in angstroms. The advantages of detecting the  $MCs^+$  molecular ions in SIMS depth profiling by  $Cs^+$  primary ions have been given by Gnaser [10], one of the most important being the minimization of the variation of ionization probabilities encountered in different matrices. The gradual decay in the  $CsN^+/Cs^+$  profiles in the two nitrided samples in Fig. 5 compared with the rapid decay in the clean Si(100) sample ( $10^{-4}$  relative count is essentially zero) indicates the presence of a nitrided  $Si_xN_y$  layer on the substrate surface. The stoichiometry of the nitride layer is of course unknown, but it is remarkable that the nitridation process occurred at room temperature. The nitrided layer by  $N_2^+$  ions appears thicker than the layer by  $N^+$  ion from the depth profiles probably because the  $N_2^+$  ion current was 5 times higher than the  $N^+$  current, even though  $N^+$  ions are much more reactive than  $N_2^+$  which must first undergo dissociation.

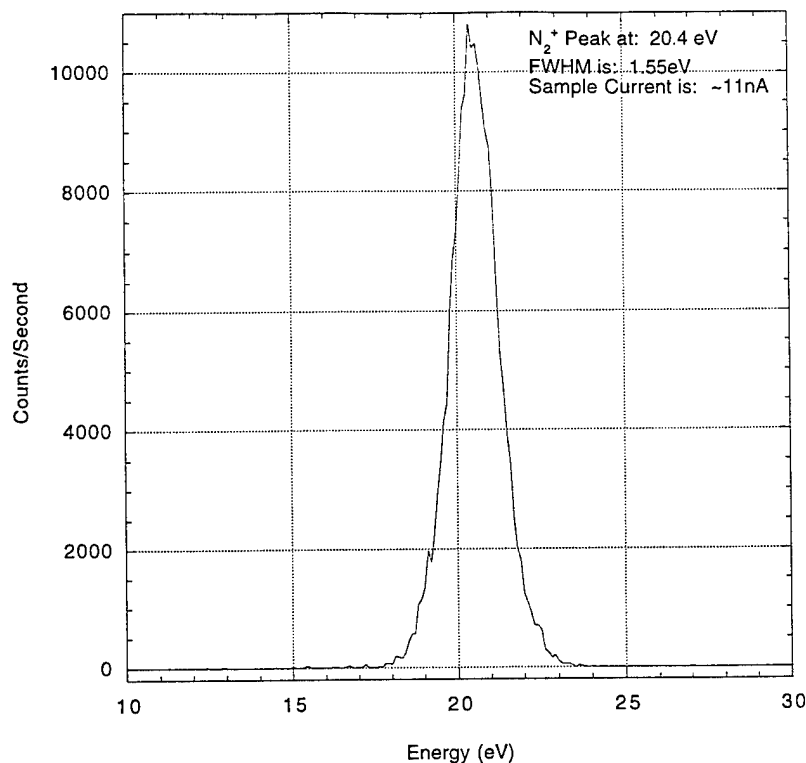


Figure 2. Typical energy distribution of  $N_2^+$  ion beam.



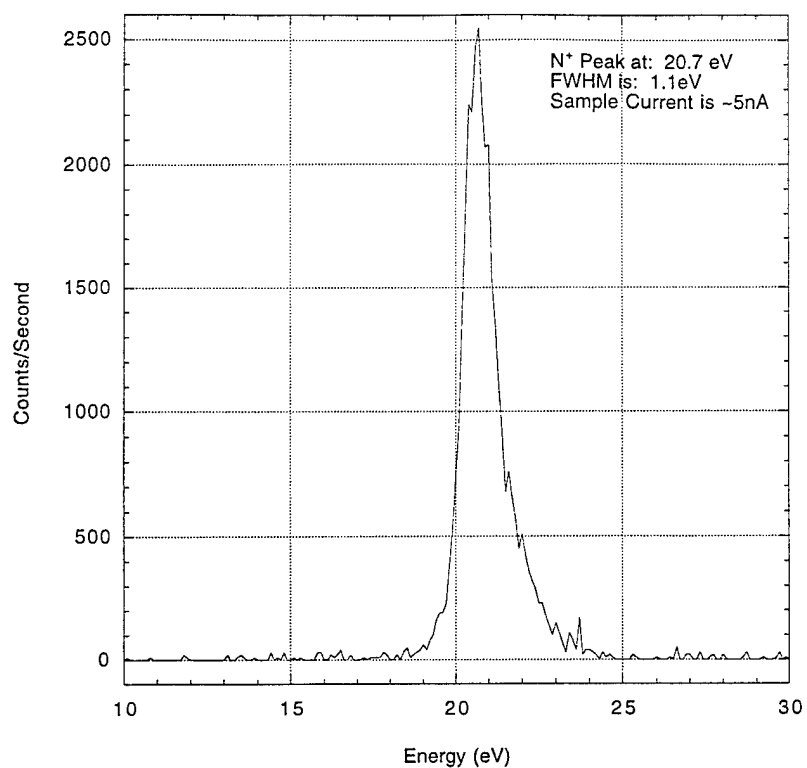


Figure 3. Typical energy distribution of  $N^+$  ion beam.

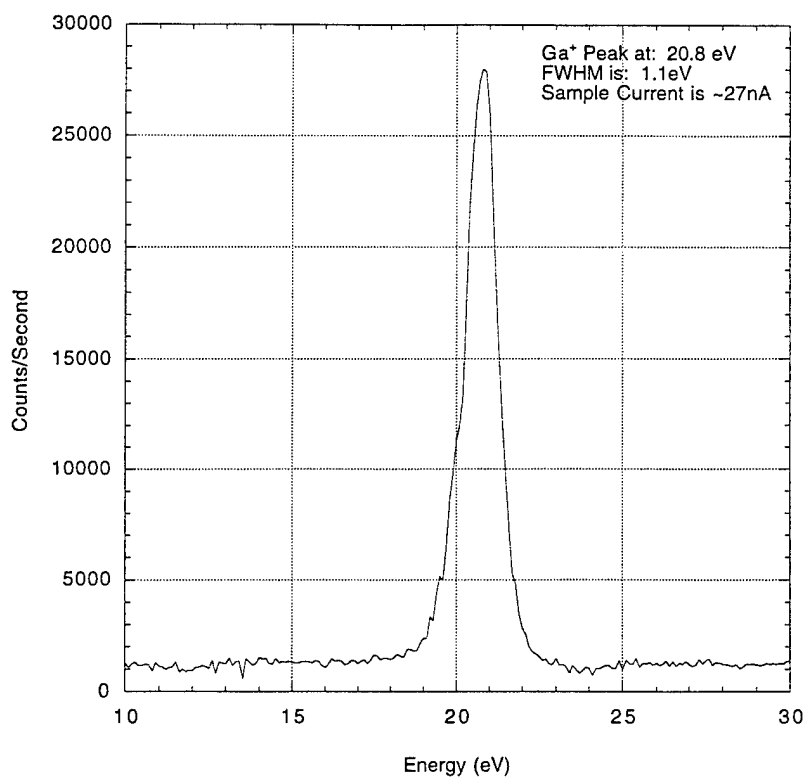


Figure 4. Typical energy distribution of the  $Ga^+$  ion beam.

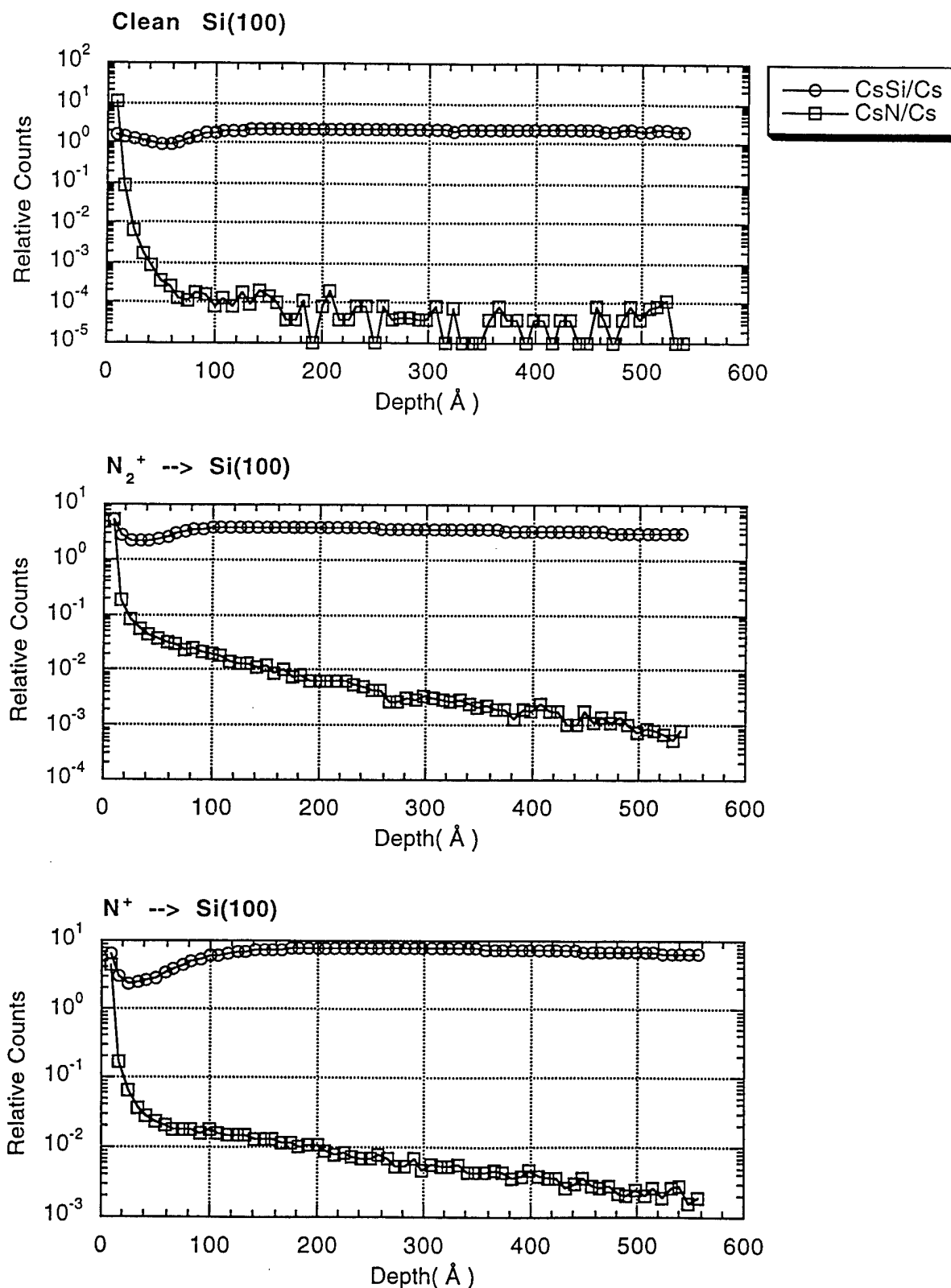


Figure 5. SIMS depth profiles showing the nitridation of Si(100) surfaces by low-energy ion beams. Normalized  $\text{CsSi}^+$  and  $\text{CsN}^+$  secondary ion signals from: a clean non-irradiated Si(100) sample (top); 38 eV  $\text{N}_2^+$  ions at 40 nA deposited on Si(100) (middle); and 40 eV  $\text{N}^+$  ions at 8 nA deposited on Si(100) (bottom).

The result of codepositing  $\text{Ga}^+$  and  $\text{N}_2^+$  ions at  $\sim 20$  eV are shown in the SIMS depth profiles in Fig. 6.  $\text{N}_2^+$  ions were chosen instead of  $\text{N}^+$  ions because of the higher flux available. The  $\text{CsGaN}^+/\text{Cs}^+$  and  $\text{CsN}^+/\text{Cs}^+$  profiles suggest the existence of a surface layer containing both Ga and N, perhaps a GaN compound film. It is interesting to note that recoil mixing effect of Ga in the Si substrates is quite severe as judged from the  $\text{CsGa}^+/\text{Cs}^+$  signal profile. The bottom depth-profile plot of Fig. 6 was taken on a thick ( $0.25\text{ }\mu\text{m}$ ) GaN film grown on sapphire by the MOCVD technique, and is included for comparison. It is remarkable that codeposition of  $\text{Ga}^+$  and  $\text{N}_2^+$  from our dual Colutron ion-beam system results in a GaN-like layer on the Si substrate given the deposition took place at room temperature. By contrast, growth of GaN films by MOCVD typically takes place at  $\sim 1000^\circ\text{C}$  while growth by MBE takes place at  $\sim 750^\circ\text{C}$ .

#### D. Conclusions

We have designed and constructed a dual Colutron ion-beam deposition system for the purpose of conducting epitaxial growth of wide bandgap compound semiconductors such as the Group III nitrides. We have demonstrated the capability of the system by codepositing both  $\text{Ga}^+$  and  $\text{N}_2^+$  ions at 20 eV on Si substrates. While the SIMS depth profiles cannot positively confirm that a GaN layer has been grown, it is nevertheless encouraging to detect both Ga and N species on the substrates. The next step will be to conduct codeposition at substrate temperatures up to  $\sim 700^\circ\text{C}$  and to conduct in situ structural analysis using RHEED and LEED on the grown films in the deposition system.

#### E. Acknowledgment

We thank U. Knipping and D. Movrin for their assistance in the laboratory and we thank R. Hervig for performing SIMS depth-profiling on our samples. This work was supported by the Office of Naval Research under grant N00014-95-1-0122, and the National Science Foundation (NSF-MRSEC) under grant DMR-9632635.

#### F. References

1. S. Strite and H. Morkoc, *J. Vac. Sci. Technol. B* 10 (1992) 1237.
2. S. Nakamura, *J. Cryst. Growth* 170 (1997) 11.
3. H. Morkoc, S. Strite, G.B. Gao, M.E. Lin, B. Sverdlov and M. Burns, *J. Appl. Phys.* 76 (1994) 1363.
4. B.R. Appleton, S.J. Pennycook, R.A. Zuhr, N. Herbots and T.S. Noggle, *Nucl. Instr. Meth. B* 19/20 (1987) 975.
5. R.A. Zuhr, B.R. Appleton, N. Herbots, B.C. Larson, T.S. Noggle and S.J. Pennycook, *J. Vac. Sci. Technol. A* 5 (1987) 2135.
6. A.H. Al-Bayati, S.S. Todorov, K.J. Boyd, D. Marton, J.W. Rabalais and J. Kulik, *J. Vac. Sci. Technol. B* 13 (1995) 1639.
7. J.W. Rabalais, A.H. Al-Bayati, K.J. Boyd, D. Marton, J. Kulik, Z. Zhang and W.K. Chu, *Phys. Rev. B* 53 (1996) 10781.
8. D.K. Brice, J.Y. Tsao and S.T. Picraux, *Nucl. Instr. Meth. B* 44 (1989) 68.

9. Colutron Research Corp., 2321 Yarmouth, Boulder, CO 80301, USA.
10. H. Gnaser, J. Vac. Sci. Technol. A12 (1994) 452.

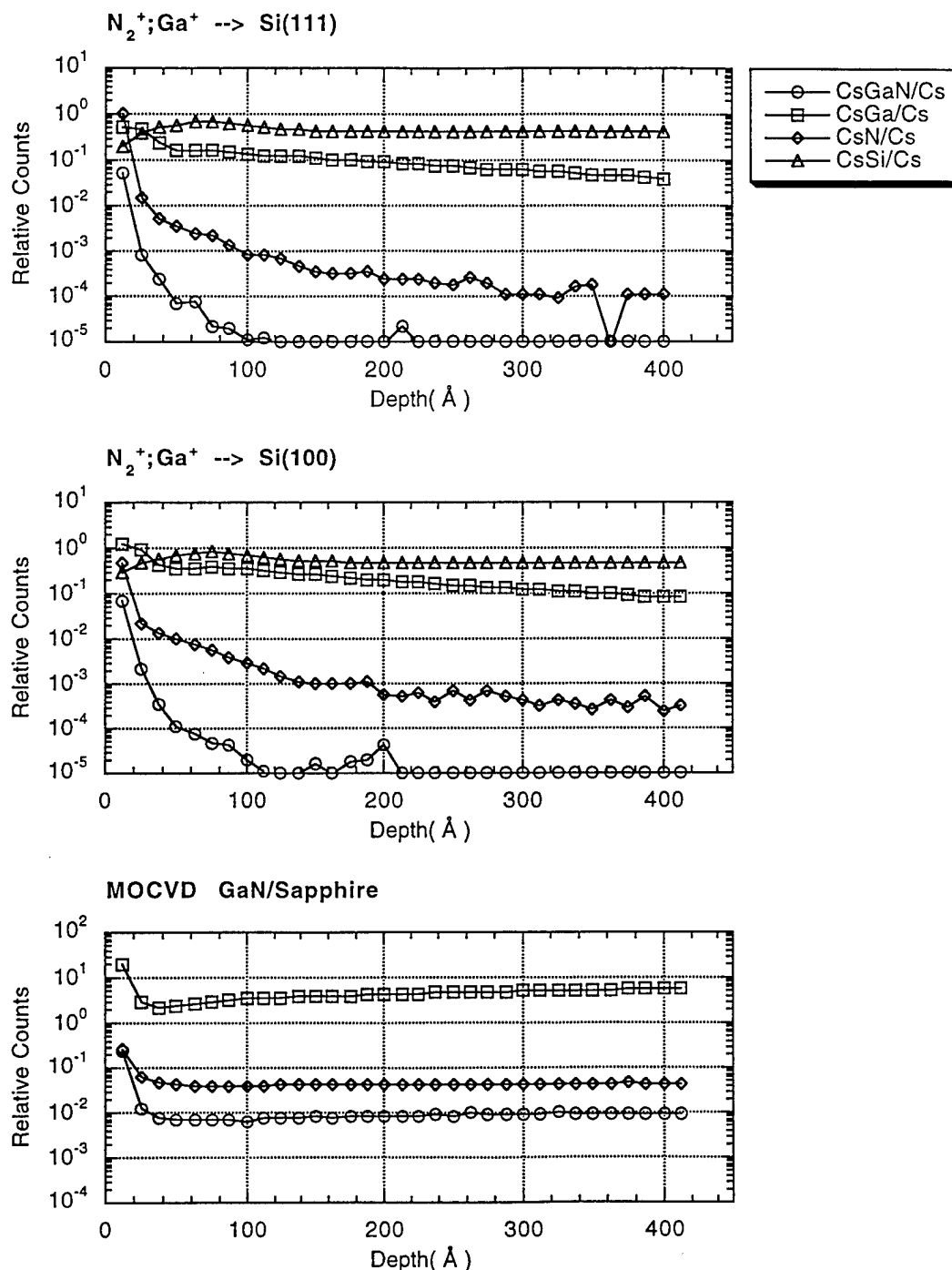


Figure 6. SIMS depth profiles showing codeposition of low-energy  $Ga^+$  and  $N_2^+$  ions on Si(111) and Si(100) surfaces. Normalized  $CsGaN^+$ ,  $CsGa^+$ ,  $CsN^+$ , and  $CsSi^+$  secondary ion signals from: 19.9 eV  $Ga^+$  and 19.4 eV  $N_2^+$  ions codeposited on a Si(111) wafer (top); 20.4 eV  $Ga^+$  and 18.8 eV  $N_2^+$  ions codeposited on a Si(100) wafer (middle); and a GaN film grown by MOCVD on a sapphire substrate (bottom).

## VII. Arc-Heated Supersonic Free-Jet of Nitrogen Atoms for the Growth of GaN, AlN and InN Thin Films

### A. Introduction

Molecular beam energies in the 1960's could be classified into two categories: (i) energies below 1 eV produced by oven-heated sources, and (ii) energies above 20 eV generated by ion beam sources. The upper limit of the former method is set by the melting temperature of the oven material and generally produces a beam with a broad energy spectrum. The lower limit of the latter technique is determined by the electrostatic repulsion of the ions, which leads to lower beam intensities. As suggested by Fenn and Anderson [1] a combination of a supersonic expansion, utilizing the narrow energy distribution, and the seeding of a heavier species into a light carrier gas leads to the availability of a high energy heavy-particle beam with narrow energy distribution. Young *et al.* [2] combined this technique with a high-temperature arc-heated jet to generate an Argon beam of energies up to 21 eV. Bickes *et al.* [3] then seeded nitrogen into argon to produce an atomic nitrogen beam with intensity  $>10^{17}$  atoms/sr/sec. These high intensity, high energy beams were used in the 1970s and 1980s for crossed molecular beam scattering experiments. At the same time lower power sources, such as the Corona discharge source [4,5], were utilized in similar experiments. In this decade, these sources seem to offer the potential in the III-V nitrides growth studies.

### B. Experimental Procedure

Advantageous features of the second generation arc source over the old source include: (i) no alignment of the tip and the nozzle being necessary, (ii) a main housing is made of Teflon with a quartz glass insert and windows cut into the sides, allowing the observation of the discharge and the tip *in situ*, (iii) tip and nozzle design which allows them to be changed while the main body source remains inside the chamber, greatly reducing the turn-around time for this procedure, (iv) greatly facilitated turn-on procedure. Like the old source, it can be run in a glow discharge mode or an arc mode resulting in different activated species.

The inexpensive (ca. \$50) corona discharge source has been built and successfully tested (Fig.1). The design of the source was based on that of Engelking [4,5]; a 4 mm Pyrex tube was drawn to closure and ground back, to form a  $94\mu\text{m}$  nozzle diameter. A tungsten wire was etched to a fine tip and secured inside the glass tube by epoxy. The glass tube was mounted to a union tee fitting and attached to a UHV flange. Typical source parameters were: nozzle pressure of 150 Torr, voltage of 5 kV, and a current of 4 mA, using the same 8% nitrogen in argon mixture as for the arc-heated source. Optical spectroscopy on both the Corona discharge source and the arc source were performed head-on using a Jarrell-Ash, 0.5m Ebert monochromator.

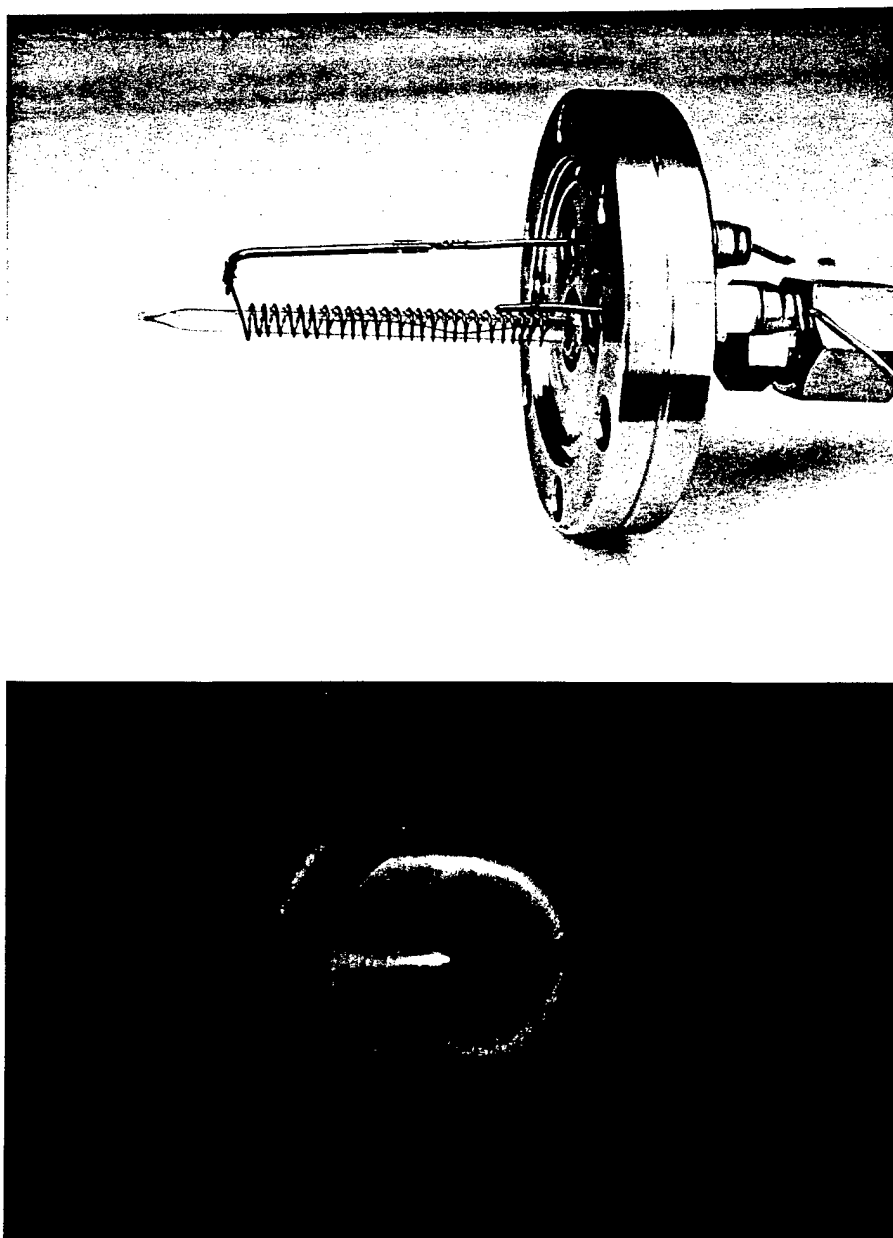


Figure 1. Corona discharge source mounted to a standard 2 3/4" UHV flange.

### C. Results and Discussion

The emitted intensities of the two sources were too low for spatially resolved optical spectra transverse to the beam axis with the current optics. Hence, optical measurements were made only with the monochromator looking directly upstream (integrating along the beam axis). Interpretation of these spectra using the current unfocused optical system was complicated by mediocre resolution, electronic noise during the amplification, and variation of background intensities. The spectra for the corona discharge source showed evidence of various excited molecular nitrogen species but very little atomic nitrogen. On the other hand, the arc source showed excited molecular nitrogen, atomic nitrogen, ionized argon and ionized molecular

nitrogen. Care must be taken in the assessment of these spectra because the integration along the expansion zone reflects primarily the hottest region of the plasma. Within the expansion, ionized species will recombine, highly excited states will cascade down to metastable states, metastable pooling can occur, as well as radiation trapping, making spatially resolved spectroscopy of the plume (the plasma expansion) a necessity. A new optical system has been designed along with a better data acquisition system that should improve the resolution and signal-to-noise level resulting in more accurate spectra, and therefore giving information on the population distribution of activated nitrogen in the expansion of the various discharge sources.

#### D. Conclusion

An improved arc source has been constructed and tested, facilitating greatly the operation and maintenance of this source. A Corona discharge source has been built, and proved to produce excited molecular nitrogen. It will, therefore, complement the arc source, where production of atomic nitrogen is predominant. Preliminary spectra were obtained for both sources; the new optical set-up will substantially improve the assessment of the diverse sources.

#### E. Future Work

After obtaining the spatially resolved spectra for both sources, and for the different modes, Time-of-flight characterization of the sources will start, along with growth studies.

#### F. References

1. J. B. Anderson and J. B. Fenn, *Phys. Fluids* **8**, 780 (1965).
2. W. S. Young, W. E. Rogers and E. L. Knuth, *Rev. Sci. Instrum.* **40**, 1346 (1969).
3. R. W. Bickes, K. R. Newton, J. M. Herrmann and R. B. Bernstein, *J. Chem. Phys.* **64**, 3648 (1976).
4. A. T. Droege and P. C. Engelking, *Chem. Phys. Letters* **96**, 316 (1983).
5. P. C. Engelking, *Rev.Sci.Instrum.* **57**, 2274 (1986).

## VIII. Distribution List

Dr. Colin Wood Office of Naval Research Electronics Division, Code: 312 Ballston Tower One 800 N. Quincy Street Arlington, VA 22217-5660	3
Administrative Contracting Officer Office of Naval Research Regional Office Atlanta 100 Alabama Street, Suite 4R15 Atlanta, GA 30303	1
Director, Naval Research Laboratory ATTN: Code 2627 Washington, DC 20375	1
Defense Technical Information Center 8725 John J. Kingman Road, Suite 0944 Ft. Belvoir, VA 22060-6218	2